Galacto-oligosaccharides as an anti-bacterial and anti-invasive agent in lung infections

Yang Cai [a], Jos P.M. van Putten [b], Myrthe S. Gilbert [c], Walter J.J. Gerrits [c], Gert Folkerts [a], Saskia Braber [a],*

[a] Division of Pharmacology, Utrecht Institute for Pharmaceutical Sciences, Faculty of Science, Utrecht University, 3584 CG, Utrecht, the Netherlands
[b] Department of Infectious Diseases and Immunology, Utrecht University, 3584 CL, Utrecht, the Netherlands
[c] Animal Nutrition Group, Wageningen University, 6700 AH, Wageningen, the Netherlands

ARTICLE INFO

ABSTRACT

Emerging antimicrobial resistance in infections asks for novel intervention strategies. Galacto-oligosaccharides (GOS) might be attractive alternatives to antibiotics due to their anti-inflammatory and anti-adhesive properties. *Mannheimia haemolytica* is one of the major *Pasteurellaceae* associated with bovine lung infections. Using *M. haemolytica*, we demonstrated that GOS have the capacity to reduce bacterial viability and can be used as adjuvant to improve antibiotic efficacy. Using *M. haemolytica*-treated primary bronchial epithelial cells (PBECs) of calves, we identified the anti-adhesive and anti-invasive activities of GOS. The observed inhibition of cytokine/chemokine release and the prevention of airway epithelial barrier dysfunction in *M. haemolytica*-treated PBECs by GOS might be related to the downregulation of "toll-like receptor 4/nuclear factor-κB" pathway and the anti-invasive and anti-adhesive properties of GOS. Particularly, GOS lowered lipopolysaccharides- but not flagellin-induced cytokine/chemokine release in calf and human airway epithelial cells. Finally, we performed *in vivo* experiments in calves and demonstrated for the first time that intranasal application of GOS can relieve lung infections/inflammation and lower *M. haemolytica* positivity in the lungs without affecting clinical performance. These findings not only shed light on the anti-inflammatory mechanisms of GOS during lung infections, but GOS might also be a promising anti-bacterial agent for preventing (lung) infections.

1. Introduction

Lung infections caused by bacteria are a common health problem in all domestic animal species as well as in humans. Pneumonia alone is responsible for more than 1.3 million child deaths annually [1]. Respiratory pathogens can successfully colonize the epithelial lining of the upper respiratory tract, grow on the mucosal surface, escape from the host immune response, and spread to a susceptible host [1,2]. These pathogens may invade the lower respiratory tract and induce infections in susceptible hosts with a weakened immune system and/or environmental stress, including adverse climatic conditions, crowding and indoor air pollution, which can serve as cofactors in the pathogenesis of lung infections [2]. The calf is considered to be a valuable animal for studying lung infections: infections are well-characterized with easy-to-observe clinical manifestations (e.g., cough reflex) and the natural incidence of pneumonia is extremely high, involving the most important airborne and close contact transmission [2,3].

Mannheimia haemolytica is a Gram-negative bacterium and is one of the major *Pasteurellaceae* associated with bovine lung infections [4,5]. *M. haemolytica* can colonize the upper respiratory tract and replicate explosively, invade deeper into the lower respiratory tract and infect lung epithelial cells [2,6]. *M. haemolytica* can impair the airway epithelial barrier integrity and induce proinflammatory mediator release, which causes an acceleration of invasion. For example, *M. haemolytica*-derived lipopolysaccharide (LPS), a potent virulence factor, can activate the toll-like receptor 4/nuclear factor-κB (TLR4/NF-κB) pathway, leading to IL-8 and IL-6 release [6–8]. In recent years, emerging antimicrobial resistance in respiratory pathogens asks for novel antimicrobial agents.

Non-digestible oligosaccharides (NDOs) are widely used carbohydrate-based biomaterials with excellent biocompatibility and biodegradability [9], in which galacto-oligosaccharides (GOS) are attractive candidates in the intervention of respiratory diseases due to their anti-inflammatory, immunomodulatory and anti-adhesive

properties [10,11]. Oral administration of NDO mixtures containing GOS and long-chain fructo-oligosaccharides (FOS) (9:1) reduced, especially respiratory, infections in the first six months of life [12], and decreased the frequency of respiratory infections, fever, and antibiotic use during the first two years of life [13]. In addition to the indirect effects of reducing respiratory infections (e.g., via the gut-lung axis) [14], we recently showed that NDOs can also be used as a direct anti-bacterial agent [10], for instance, GOS and alginate-oligosaccharides can decrease the growth of *Escherichia coli in vitro* [15].

Here, we hypothesized that GOS may alleviate lung infection-induced inflammation *ex vivo* and *in vivo*. We demonstrated that GOS can lower *M. haemolytica* viability and enhance antibiotic efficacy, possibly related to the damaged bacterial membrane integrity. We showed for the first time that intranasal GOS lowered airway inflammation in calves with naturally acquired lung infections, which might be related to the interesting findings that GOS inhibited *M. haemolytica* growth as well as prevented *M. haemolytica* from invading primary bronchial epithelial cells (PBECs) and from disrupting the airway epithelial integrity. NDOs, such as GOS, with or without the combination of antibiotics might be helpful in resisting inflammation caused by lung infections and we innovatively propose a new route of administration (intranasal application) for NDOs to treat these infections.

2. Results

2.1. Effect of GOS on the growth of M. haemolytica in vitro

GOS are produced by conversion of lactose using the enzyme β-galactosidase and consist of a mixture of mainly DP2-6 built up of galactose and glucose units in various arrangements (Fig. 1A and Supplementary Table S1) [16–18].

M. haemolytica (1×10^5 CFU/mL, initial CFUs at 0 h) was incubated with or without increasing concentrations of GOS over time (within 24 h). Bacterial growth assays (OD600nm) in the presence of different concentrations of GOS (4%, 8%, 16%) revealed a significant concentration-dependent reduction in the growth of *M. haemolytica* (Fig. 1B). Compared with *M. haemolytica*, 4% GOS lowered the growth of *M. haemolytica* after 12 h and 24 h incubation, while no significant growth of *M. haemolytica* was observed in 8% and 16% GOS treatments (Fig. 1B and C). The minimum inhibitory concentration (MIC) of GOS was 8% (Fig. 1C). In addition, Supplementary Table S2 showed that different concentrations of GOS did not change the pH of the medium after 24 h incubation in the absence of *M. haemolytica*.

In order to determine whether GOS was bacteriostatic or bactericidal, supernatants from GOS-treated *M. haemolytica* were sub-cultured onto sheep blood agar plates (Fig. 1D). *M. haemolytica* treated with 8% and 16% GOS for 24 h exhibited significant lower CFU/mL compared to *M. haemolytica* alone at 24 h. In addition, the CFUs of 8% and 16% GOS treatment were 7950 and 525 CFU/mL, respectively, which were 92.1% and 99.5% lower than the initial CFUs of *M. haemolytica* (1×10^5 CFU/mL; Fig. 1D). The live/dead ratio was measured for *M. haemolytica* with or without GOS treatment. Compared to *M. haemolytica* at 0 h, the live/dead ratio of *M. haemolytica* at 24 h did not significantly change (Fig. 1E). The live/dead ratio of *M. haemolytica* at 0 h and 24 h is close to 4, while 4%, 8% and 16% GOS-treated *M. haemolytica* showed lower ratios (Fig. 1F). Especially, 8% and 16% GOS-treated *M. haemolytica* showed live/dead ratios lower than 0.3, indicating that the vast majority of *M. haemolytica* was dead after GOS incubation.

M. haemolytica (1×10^5 CFU/mL, initial CFUs at 0 h) were sub-cultured onto GOS-coated blood agar plates. Compared with uncoated plates, 8% and 16% GOS-coating significantly reduced *M. haemolytica* CFUs by 87% and 97%, respectively (Fig. 1G).

2.2. GOS increase the efficacy of antimicrobial drugs against M. haemolytica

β-lactams (e.g., ampicillin), tetracycline (e.g., doxycycline, oxytetracycline) and macrolide (e.g., tilmicosin) are widely used to treat respiratory diseases in calves, especially in *M. haemolytica*-induced lung infections [19]. *M. haemolytica* was incubated with increasing concentrations of ampicillin, doxycycline, oxytetracycline and tilmicosin for 24 h to evaluate the MIC. The MIC of ampicillin against *M. haemolytica* was 0.032 µg/mL and the MIC of doxycycline, oxytetracycline and tilmicosin was 0.512 µg/mL (Fig. 2A–D). GOS (4%) were combined with these antimicrobial drugs to investigate the additive anti-bacterial effect. As shown in Fig. 2E, the combination of GOS with ampicillin (4% + 0.016 µg/mL) was more efficient in inhibiting *M. haemolytica* growth as compared to GOS or ampicillin alone. In addition, 4% GOS lowered the MIC of doxycycline from 0.512 to 0.064 µg/mL and lowered the MIC of oxytetracycline and tilmicosin from 0.512 to 0.032 µg/mL (Fig. 2F–H).

To learn more about the mode of action of GOS, changes in bacterial membrane potential were measured using the fluorescent membrane potential indicator dye, $DiOC_2(3)$ [20], while membrane damage was determined by staining with nucleic acid dyes, propidium iodide (PI) and SYTO9. $DiOC_2(3)$ emits green fluorescence but forms red fluorescent aggregates in the bacterial cytosol with increasing membrane potential. This effect was prevented in the presence of the proton gradient disruptor carbonyl cyanide 3-chlorophenylhydrazone (CCCP) (Fig. 2I). Interestingly, exposure of *M. haemolytica* to 4% GOS for 12 and 24 h also reduced the red/green ratio, indicating a decrease in membrane potential (Fig. 2I). In addition, live *M. haemolytica* with intact membranes (green) and dead *M. haemolytica* with damaged membranes (red) were stained with SYTO 9 and PI, respectively. As shown in Fig. 2J, 4% GOS increased the proportion of *M. haemolytica* with damaged membranes.

2.3. GOS with or without antimicrobial drugs suppress the release of IL-8 and IL-6 in a bovine PBEC infection

To better understand the effect of GOS with or without antimicrobial drugs in a more complex setting with airway epithelial cells, we isolated and cultured PBECs of healthy bovine lungs and developed an *ex vivo* infection model [8]. Compared with control, *M. haemolytica*-treated PBECs showed higher IL-8 and IL-6 concentrations (Fig. 3A and B). As expected, 4% GOS preincubation inhibited *M. haemolytica*-induced IL-8 and IL-6 release, while 4% GOS alone did not significantly affect IL-8 and IL-6 release (Fig. 3A and B).

Optimal combinations of 4% GOS with different concentrations of ampicillin, doxycycline, oxytetracycline or tilmicosin as obtained from the MIC assay depicted in Fig. 2E–H were also used as pretreatments in *M. haemolytica*-treated PBECs (Fig. 3). Doxycycline at 0.256 µg/mL (but not ampicillin at 0.016 µg/mL) lowered the *M. haemolytica*-induced IL-8 and IL-6 release (Fig. 3A and B). All combinations of 4% GOS with ampicillin (0.016 µg/mL), or 4% GOS with doxycycline (0.032–0.256 µg/mL) reduced the *M. haemolytica*-induced IL-8 and IL-6 release in PBECs. Especially, these combination treatments showed more promising effects for the inhibition of IL-8 and IL-6 release than 4% GOS, ampicillin and doxycycline alone (Fig. 3A and B). The combination of 4% GOS with oxytetracycline (0.032 µg/mL), or 4% GOS with tilmicosin (0.032 µg/mL) also showed more promising anti-inflammatory effects than 4% GOS, oxytetracycline and tilmicosin alone (Fig. 3C and D).

2.4. Anti-invasive and anti-adhesive effect of GOS in a bovine PBEC infection

GOS ≥4% may affect the PBEC viability as observed by higher LDH release and/or lower survival rate after 48 h incubation (Supplementary Figs. S1A and B), therefore anti-inflammatory effects were also tested for lower concentrations of GOS. Release of IL-8 and IL-6 induced by *M. haemolytica* was inhibited by pretreatment with 1% and 2% GOS in
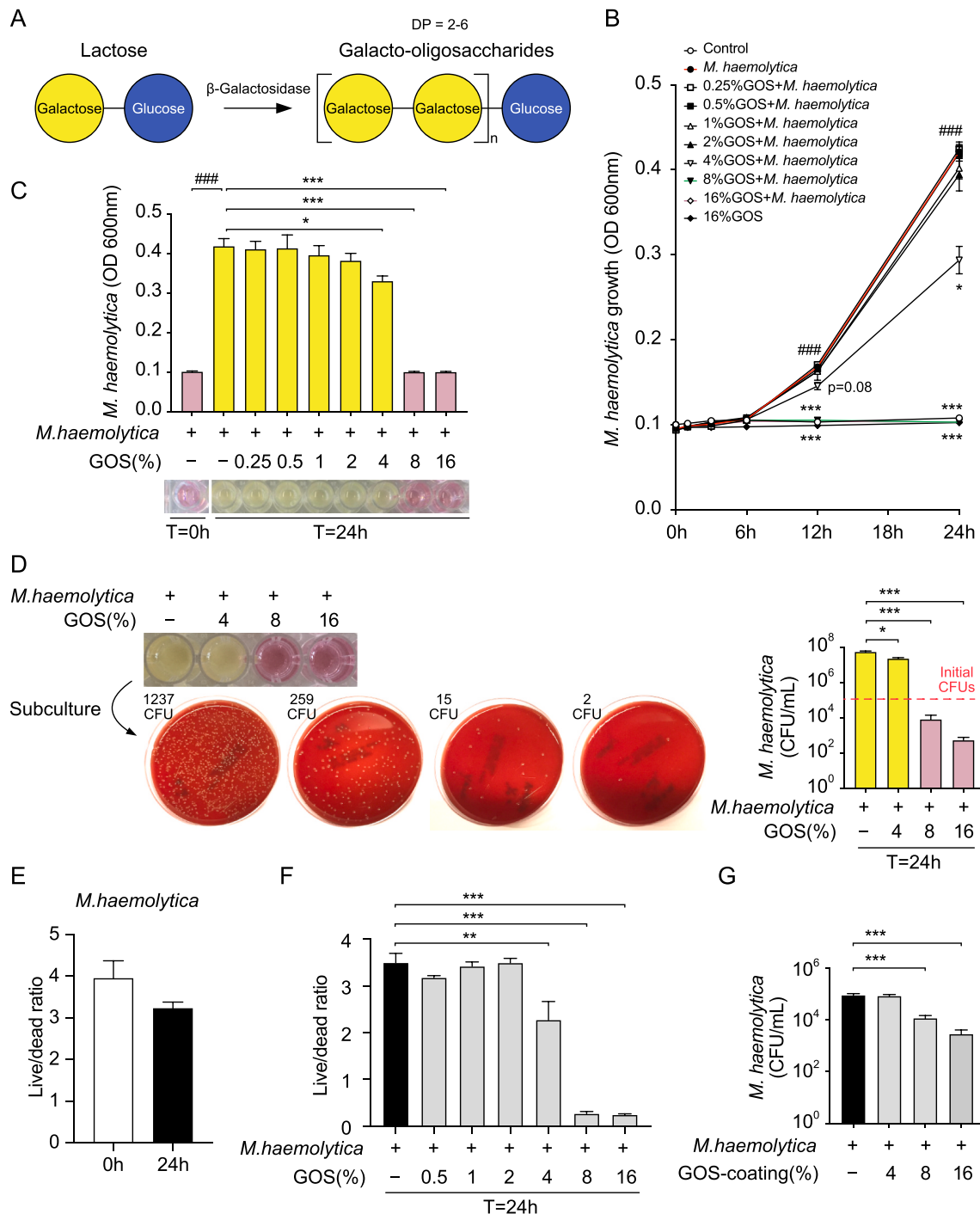
Fig. 1. Effect of GOS on the growth of *M. haemolytica in vitro*. (A) The production and representative structure of GOS. (B–D) *M. haemolytica* (1×10^5 CFU/mL) was incubated with or without increasing concentrations of GOS for 24 h, thereafter supernatants were sub-cultured onto sheep blood agar plate overnight. (B) *M. haemolytica* growth (OD600nm) was recorded at different timepoints (0, 1, 3, 6, 12 and 24 h) after incubation with or without GOS. (C) Minimum inhibitory concentration (MIC) of GOS against *M. haemolytica* was determined after 24 h incubation and assigned as the lowest concentration of compound at which no change in OD600nm value and medium color was observed. (D) *M. haemolytica* numbers were determined by counting CFUs on each agar plate and calculated as CFU/mL based on the dilution factor of 50,000 for *M. haemolytica* group and 4% GOS treatment and dilution factor of 100 for 8% and 16% treatments. (E–F) Live/dead ratio of *M. haemolytica* at 0 h and 24 h with or without the treatment of increasing concentrations of GOS were determined by a LIVE/DEAD BacLight assay. (G) *M. haemolytica* (1×10^5 CFU/mL) was diluted and sub-cultured onto sheep blood agar plate precoated with or without GOS (overnight). *M. haemolytica* numbers were determined by counting *M. haemolytica* CFUs on each agar plate and calculated as CFU/mL based on the dilution factor of 100. $\#\#\#P<0.001$ (*M. haemolytica* 12 or 24 h vs 0 h); $*P<0.05$; $**P<0.01$; $***P<0.001$ (GOS treatment vs *M. haemolytica* group at that timepoint). Data are presented as means $\pm$ SEM. All data shown are representative of at least three independent experiments (n = 3–6 bacterial generations, 1–2 generation(s) per experiment). (For interpretation of the references to color in this figure legend, the reader is referred to the Web version of this article.)
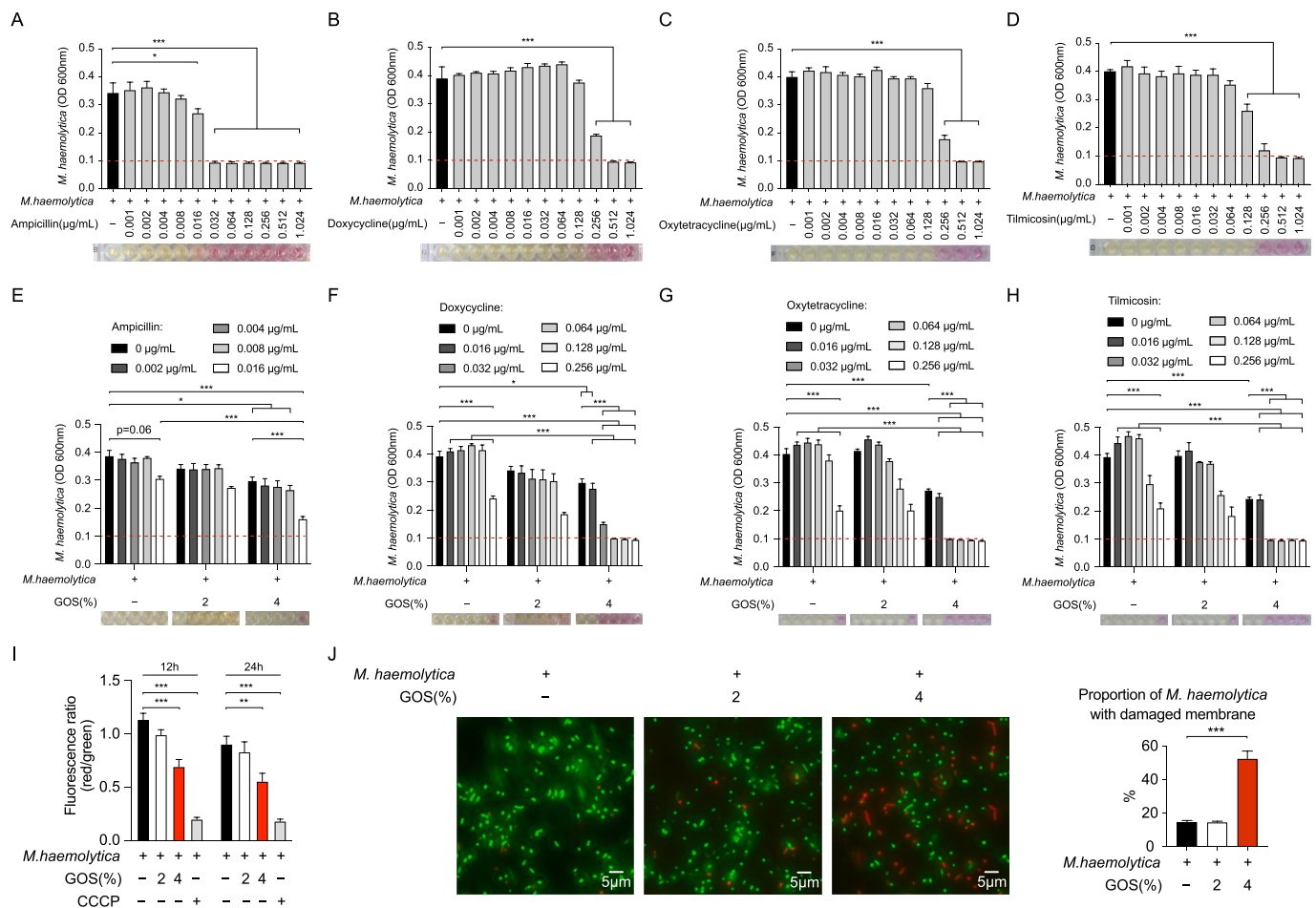
Fig. 2. GOS increase the efficacy of antimicrobial drugs against *M. haemolytica*. (A–D) *M. haemolytica* (1×10^5 CFU/mL, initial CFUs at 0 h) was incubated with increasing concentrations of ampicillin, doxycycline, oxytetracycline and tilmicosin for 24 h, thereafter *M. haemolytica* growth in the supernatants (MIC assay) was determined at OD600nm. (E–H) *M. haemolytica* was incubated with the combination of 2% or 4% GOS with ampicillin, doxycycline, oxytetracycline or tilmicosin for 24 h, thereafter *M. haemolytica* growth in the supernatants (MIC assay) was determined at OD600nm. Red dotted line shows the OD value of the medium alone. (I) *M. haemolytica* was incubated with 4% GOS for 12 and 24 h, thereafter the membrane potential of *M. haemolytica* was measured by the red/green fluorescence ratio of DiOC$_2$(3) using a bacterial membrane potential kit. CCCP was provided in the same kit and used as a depolarized control. (J) Live *M. haemolytica* with intact membranes (green) and dead *M. haemolytica* with damaged membranes (red) were stained with SYTO 9 and PI, respectively. Data were shown as proportion of *M. haemolytica* with damaged membranes. *$P < 0.05$; **$P < 0.01$; ***$P < 0.001$. Data are presented as means ± SEM. All data shown are representative of five independent experiments (n = 5 bacterial generations, one generation per experiment). (For interpretation of the references to color in this figure legend, the reader is referred to the Web version of this article.)

PBECs (Fig. 4A and B), while the cellular survival and LDH release were not affected (Fig. 4C and D).

Lower concentrations of GOS may act as anti-adhesives and decoy glycan receptors to protect host cells [10], therefore the anti-adhesive effects of GOS were investigated in the PBEC infection model. The number of *M. haemolytica* in the supernatants increased from 1×10^5 (initial CFUs) to 0.9×10^8 CFU/mL after 24 h incubation with PBECs. However, GOS at 1% and 2% did not affect the *M. haemolytica* growth in the supernatants (Fig. 4E and F). In Fig. 4G and H, the numbers of *M. haemolytica* invaded and adhered to PBECs were 0.6×10^5 and 1.5×10^5 CFU/mL, respectively. Interestingly, 2% GOS caused a significant decrease in adhesion to and invasion of (entry into) the cells by *M. haemolytica* (Fig. 4G and H).

2.5. GOS inhibit M. haemolytica-induced inflammation and barrier dysfunction in PBECs

As a consequence of the continuous adhesion to and invasion of PBECs, *M. haemolytica* is likely to impair the integrity of epithelial cell monolayers [8]. In the present study, PBECs exposed to *M. haemolytica* resulted in a significant decrease in transepithelial electrical resistance

(TEER) (Fig. 5A), which facilitated the translocation of lucifer yellow from the apical to the basolateral compartment and this coincided with the release of IL-8 and IL-6 (Fig. 5B–D). Interestingly, GOS pretreatment prevented the decreased TEER and increased lucifer yellow flux and corresponding IL-8 and IL-6 release compared to *M. haemolytica*-treated PBECs (Fig. 5A–D).

Another characteristic of *M. haemolytica*-treated airway epithelial cells is the alteration in barrier function-associated molecules [8,21]. In the present study, *M. haemolytica* exposure (24 h) resulted in a significant decrease in protein and fluorescence level of the tight junction protein ZO-1 and adherens junction protein E-cadherin in PBECs (Fig. 5E–G). Moreover, 2% GOS pretreatment prevented this reduction of ZO-1 and E-cadherin in protein level and fluorescence intensity (Fig. 5E–G).

2.6. Anti-inflammatory effect of GOS might be related to the inhibition of TLR4/NF-κB pathway

One of the potential mechanisms of *M. haemolytica*-induced inflammation is the activation of the TLR4/NF-κB signaling pathway induced by *M. haemolytica* released LPS [8]. Here, higher protein expression of
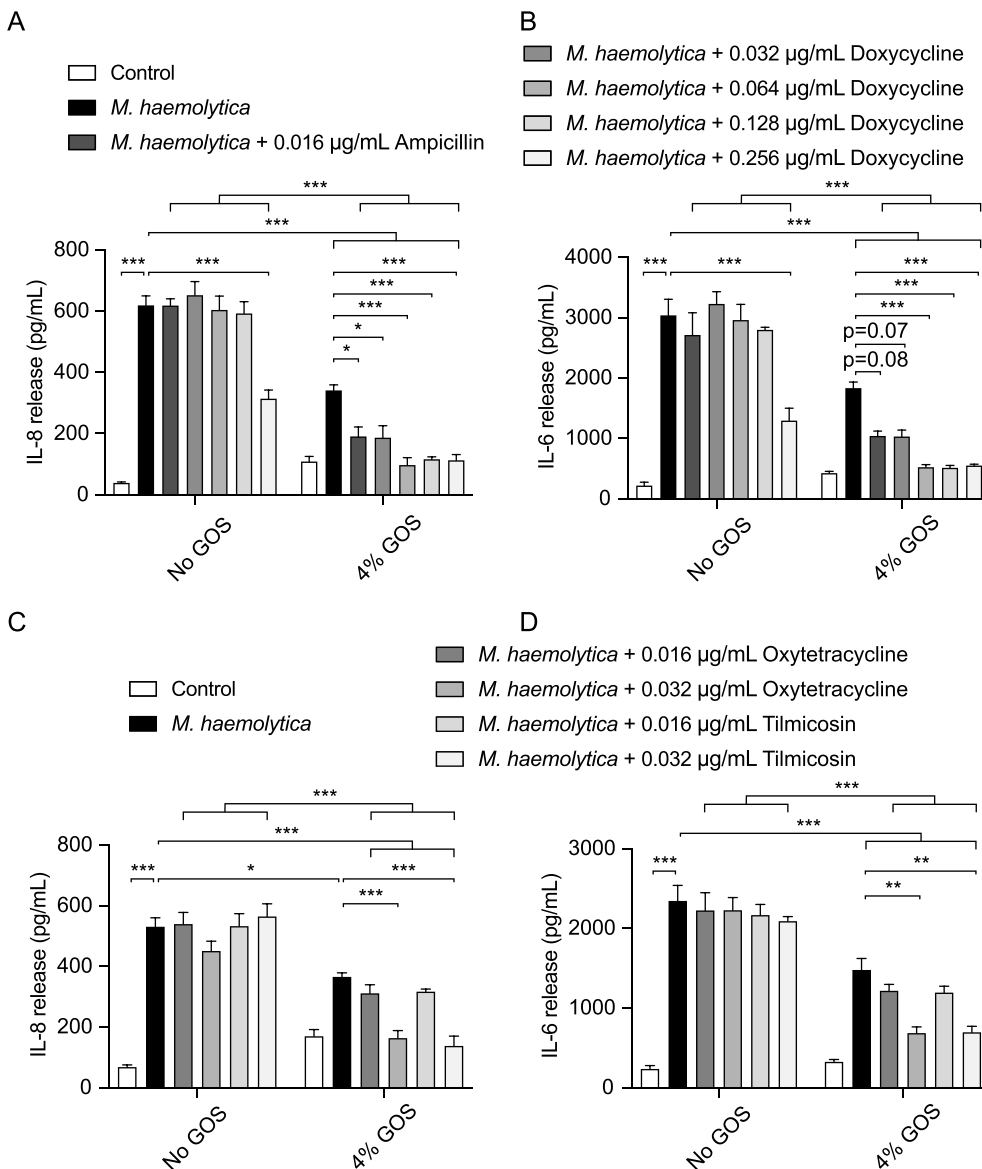
Fig. 3. GOS with or without antimicrobial drugs suppress the release of IL-8 and IL-6 in a bovine PBEC infection. PBECs were pretreated with GOS, ampicillin, doxycycline, oxytetracycline, tilmicosin, GOS + ampicillin, GOS + doxycycline, GOS + oxytetracycline, or GOS + tilmicosin for 24 h prior to the 24 h *M. haemolytica* (1×10^5 CFU/mL) exposure. (**A** and **C**) IL-8 and (**B** and **D**) IL-6 levels in the supernatants of PBECs were measured by ELISA. *P<0.05; **P<0.01; ***P<0.001. Data are presented as means ± SEM. All data shown are representative of five independent experiments (n = 5 donor calves, one donor calf per experiment).

TLR4 and phosphorylation of NF-κB p65 were observed in *M. haemolytica*-treated PBECs compared with control (Fig. 6A). Interestingly, 2% GOS pretreatment showed a lower protein expression of TLR4 and phosphorylation of NF-κB p65 in PBECs after *M. haemolytica* exposure (Fig. 6A). A TLR4 inhibitor (CLI-095) was applied to investigate whether inhibition of the TLR4/NF-κB pathway could affect *M. haemolytica*-induced inflammation. As expected, CLI-095 lowered the protein expression of TLR4, p-p65 and the release of IL-8 and IL-6 in *M. haemolytica*-treated PBECs, while CLI-095 alone had no effects (Fig. 6A–C). Although CLI-095 inhibited IL-8 and IL-6 release, it did not significantly prevent the *M. haemolytica*-induced disruption of the PBEC monolayer integrity (Supplementary Fig. S2).

To confirm the inhibition of TLR4/NF-κB pathway by GOS, a TLR4 ligand (LPS) and a TLR5 ligand (flagellin) were used as stimulants to assess the anti-inflammatory effect of GOS in both bovine and human airway epithelial cells. In line with our previous findings [8], LPS and flagellin induced the release of IL-8 and IL-6 in PBECs (Fig. 6D–G). Despite a significant inhibition in LPS-induced IL-8 and IL-6 release caused by GOS pretreatment, GOS did not significantly affect flagellin-induced IL-8 and IL-6 release (Fig. 6D–G). Furthermore, LPS/flagellin with and without GOS supplementation did not significantly affect the cellular survival and LDH release in PBECs

(Supplementary Figs. S1C and D).

Comparable to the results with the PBECs, GOS pretreatment inhibited LPS, but not flagellin-induced IL-8 and IL-6 release from human alveolar epithelial (A549) cells (Fig. 6H and I) and human bronchial epithelial (16HBE) cells (Fig. 6J and K).

2.7. Effect of intranasal application of GOS on calves with naturally occurring lung infections

Due to the interesting *in vitro* anti-bacterial, anti-adhesion and anti-inflammatory properties of GOS mentioned above, an animal experiment was conducted to investigate the anti-infective effect of intranasal GOS administration in calves. Calves were naturally exposed to respiratory pathogens in the environment (natural incidence of lung infections, animals were not challenged). GOS were intranasally administrated once per day from experimental week 1 till 8, thereafter these calves were not exposed to GOS from week 9 till 27 (Fig. 7A).

A tended increase in total cell numbers (increased by 0.92-fold; mainly pulmonary leukocytes; Supplementary Figs. S3B) and a significant increase in neutrophil and lymphocyte numbers (increased by 11-fold and 138-fold, respectively; Supplementary Figs. S3C and E) and percentages (Fig. 7E and F) were observed in bronchoalveolar lavage
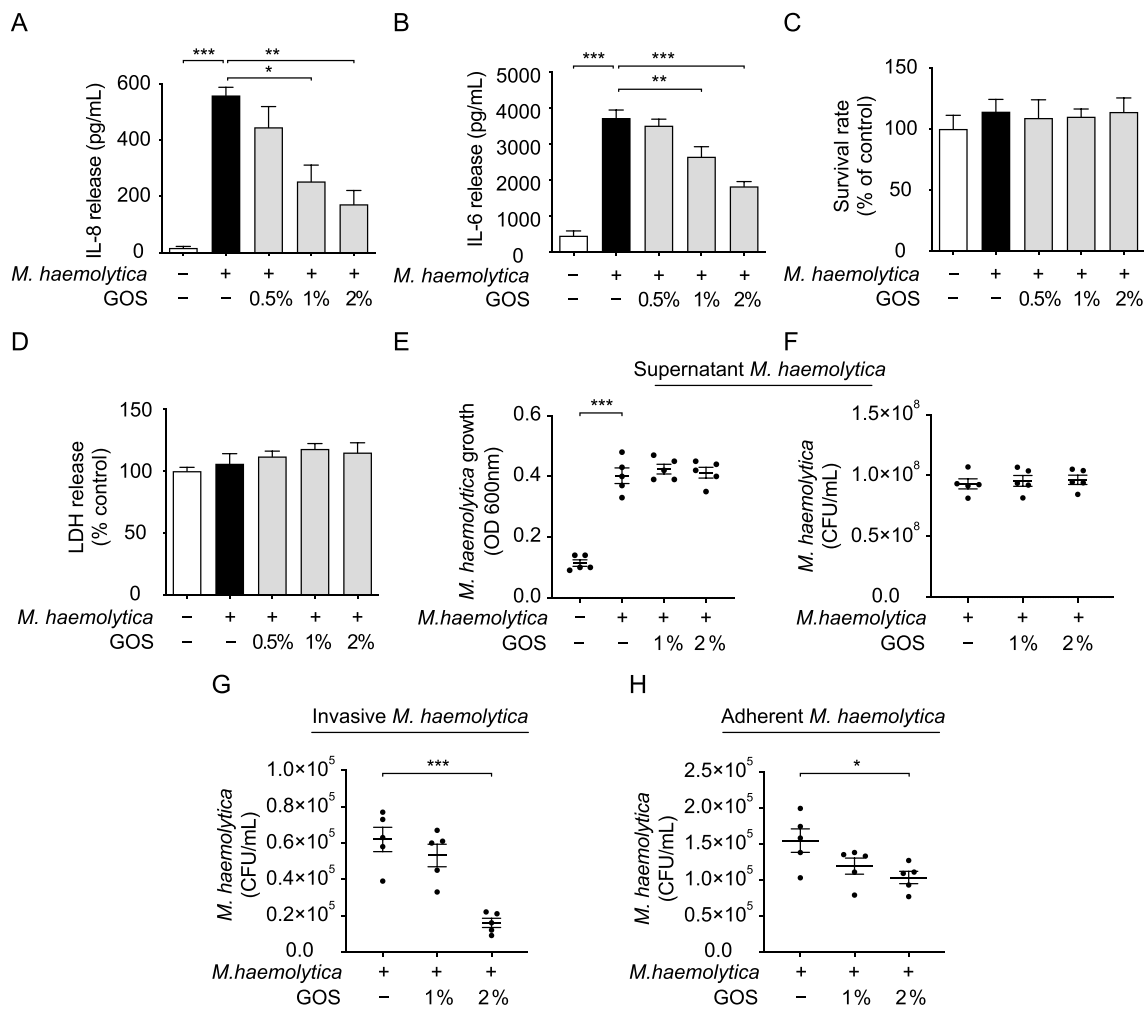
Fig. 4. Anti-invasive and anti-adhesive effect of GOS in a bovine PBEC infection. PBECs were treated with *M. haemolytica* (1×10^5 CFU/mL) for 24 h with or without 24 h GOS pretreatment, thereafter supernatants were collected and PBECs were lysed with or without supplementation of extracellular gentamicin (for killing the adherent *M. haemolytica*) and sub-cultured onto blood agar plates overnight. (**A-D**) IL-8, IL-6 and LDH release in the supernatants of PBECs and PBEC survival rates (MTT assay) were measured. (**E**) *M. haemolytica* growth in the supernatants was determined by measuring turbidity of supernatants at OD600nm. (**F**) Supernatants were sub-cultured on blood agar plate and *M. haemolytica* numbers in the supernatants were determined by counting CFUs on each agar plate and presented as CFU/mL. (**G-H**) The number of invasive (**G**) and adherent (**H**) *M. haemolytica* was determined by counting CFUs on each agar plate and presented as CFU/mL. *$P<0.05$; **$P<0.01$; ***$P<0.001$. Data are presented as means ± SEM. All data shown are representative of five independent experiments (n = 5 donor calves, one donor calves per experiment).

fluid (BALF) of control calves from week 5, compared to week 1. In contrast, a significant decrease in macrophage numbers (decreased by 56%; Supplementary Fig. S3D) and percentages (Fig. 7D) was found in BALF of control calves. From week 5, neutrophils instead of macrophages became the main type of leukocytes in BALF of control calves as shown in the representative cytospins (Fig. 7C). At week 6, the blood leukocytes were increased by 26% in comparison with week 0 (baseline) (Fig. 7G and Supplementary Fig. S3A). In addition, the clinical scores continuously increased over time and reached peak scores at week 6 (Fig. 7B). These findings indicate that lung infections were present in these calves from week 5.

Although no effects on the clinical scores, BALF total cell numbers, and BALF lymphocytes over time (Fig. 7B, F and Supplementary Figs. S3B and C), intranasal GOS elevated the percentages and numbers of macrophages (Fig. 7C and D and Supplementary Fig. S3D) and lowered the percentages and numbers of neutrophils (Fig. 7C, E and Supplementary Fig. S3E) in BALF at week 5, compared to control calves. After 6 weeks of intranasal administration, GOS prevented the increase of leukocytes in blood (Fig. 7G and Supplementary Fig. S3A).

The inflammatory response in the lungs was investigated by measuring cytokines/chemokines in BALF. TNF-α concentrations of

control calves increased significantly over time and reached the highest-level during week 5 (Supplementary Fig. S3F). As expected, intranasal GOS suppressed TNF-α levels in BALF at week 5 (Fig. 7I and Supplementary Fig. S3F). In addition, other chemokine/cytokine (i.e., IL-8, IL-6 and IL-1β) levels were also measured during week 5, indicated as the timepoint for lung infections. Intranasal GOS significantly reduced the concentrations of IL-6 and IL-1β (Fig. 7J and K), but not IL-8 at week 5 (Fig. 7H). The same cytokines/chemokines were analyzed in blood to investigate the effect of intranasal GOS on systemic inflammation caused by lung infections at week 4 and 6 (one week prior to or one week after week 5). Intranasal GOS significantly lowered the blood concentrations of IL-6 and IL-1β at week 4, but not at week 6, while no significant effects on IL-8 and TNF-α levels were observed (Fig. 7L–O).

At week 27, the right cranial lung lobe was collected after slaughter and stained with hematoxylin-eosin (HE). As shown in Fig. 7P, the lung lesions were still observed in these calves after natural exposure for 27 weeks and demonstrated collapsed alveoli or thickened alveolar septa, hyperplasia of bronchus or bronchioles, infiltration of inflammatory cells, and/or diapedesis of erythrocytes. Interestingly, calves received intranasal GOS administration for 8 weeks exhibited lower histopathological lung scores compared to control calves (Fig. 7P).
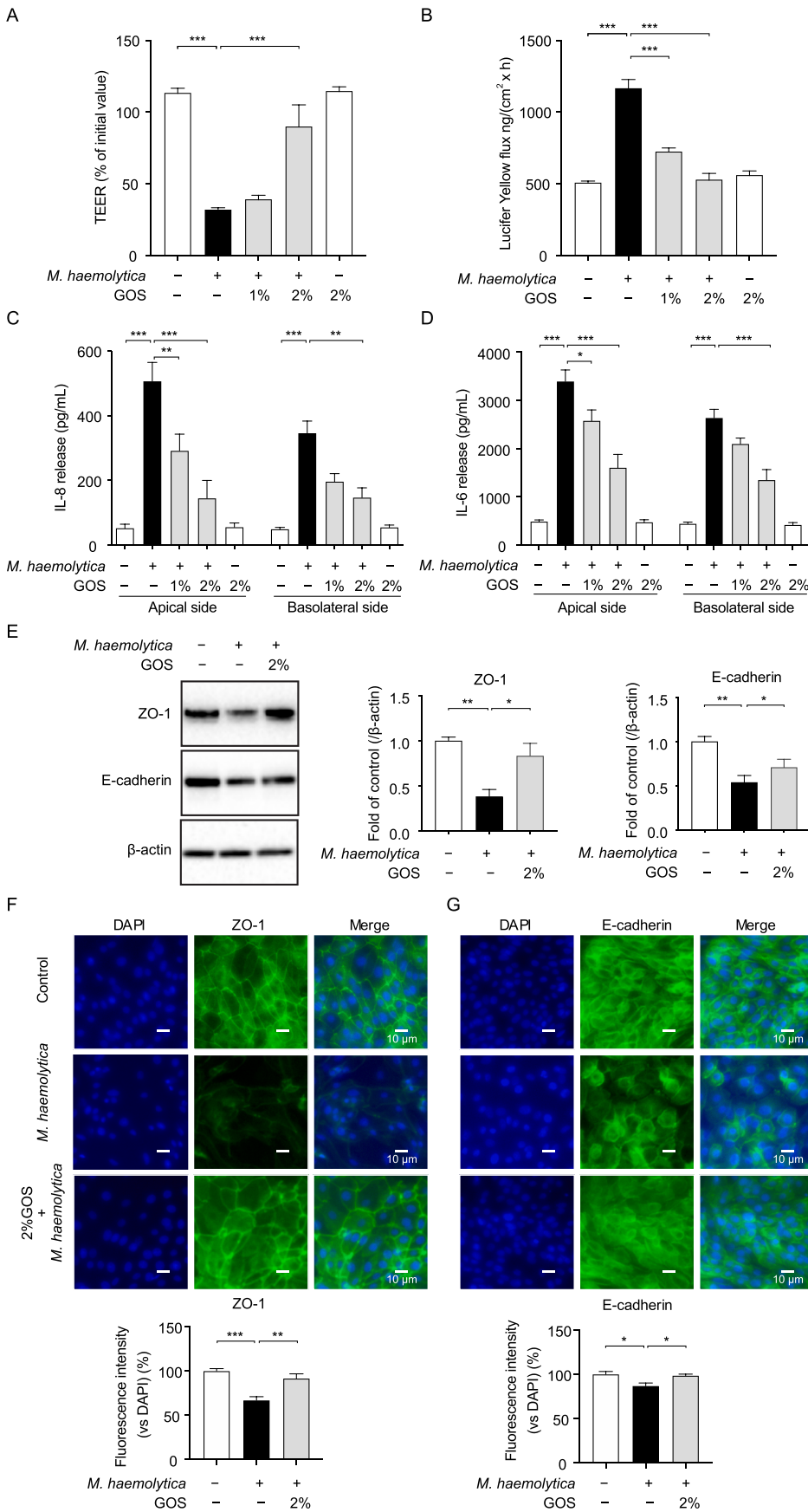
Fig. 5. GOS inhibit _M. haemolytica_-induced inflammation and barrier dysfunction in PBECs. PBECs were incubated with _M. haemolytica_ (1×10^5 CFU/mL) for 24 h with or without 24 h pretreatment with GOS. After incubation, (**A**) TEER was measured and (**B**) lucifer yellow flux from apical to basolateral compartment was determined. (**C**–**D**) The release of IL-8 and IL-6 in both apical and basolateral compartment was assessed by ELISA. (**E**) The immunoblots were obtained with ZO-1, E-cadherin and β-actin (protein loading control) (original blots are depicted in Supplementary Fig. S4A). (**F**–**G**) Cellular expression of ZO-1 and E-cadherin in PBECs was assessed by immunofluorescent staining and quantified as a percentage of fluorescence intensity. *_P_<0.05; **_P_<0.01; ***_P_<0.001. Data are presented as means ± SEM. All data shown are representative of five independent experiments (n = 5 donor calves, one donor calf per experiment). (For interpretation of the references to color in this figure legend, the reader is referred to the Web version of this article.)
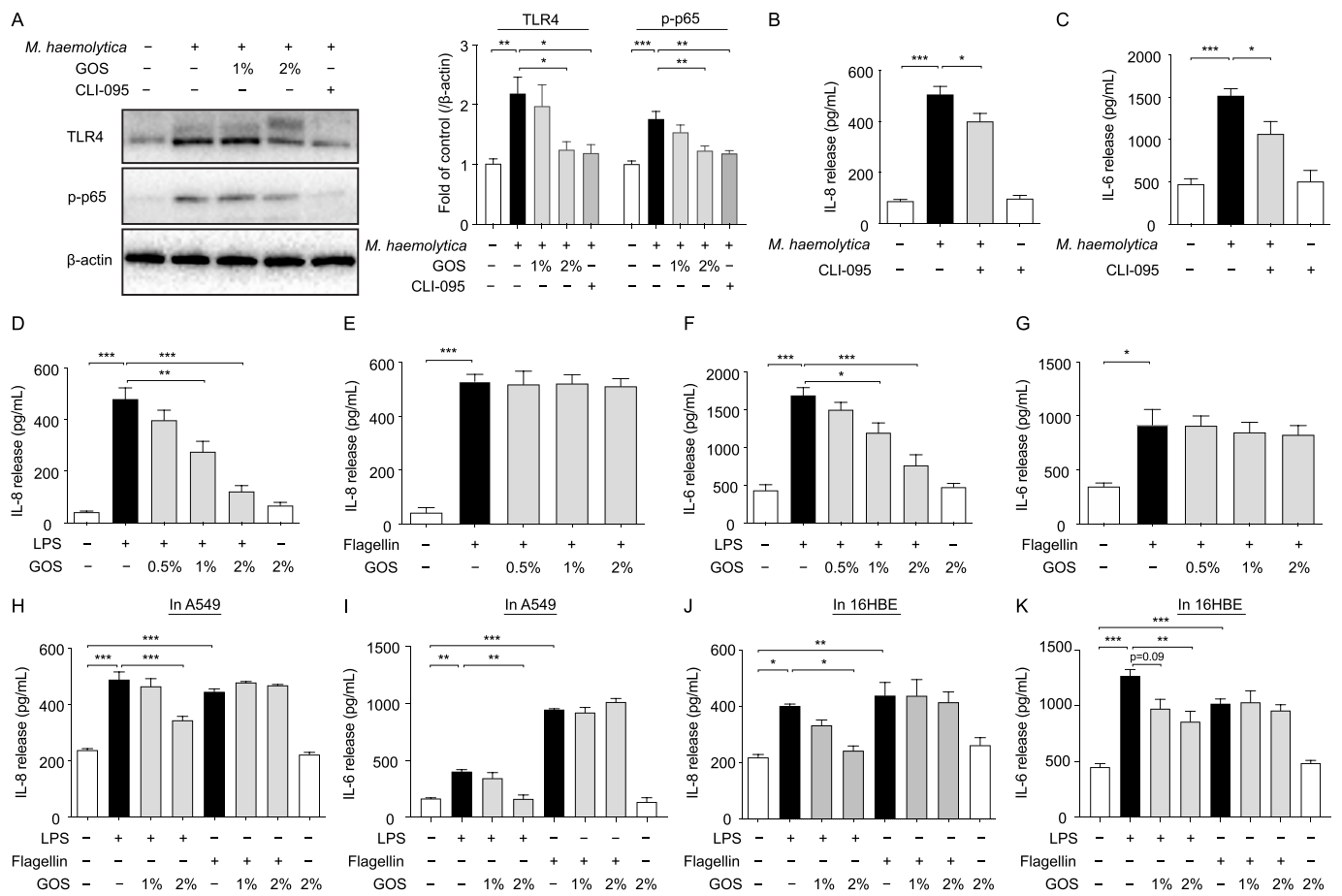
Fig. 6. Anti-inflammatory effect of GOS might be related to the inhibition of TLR4/NF-κB pathway. (A–C) PBECs were incubated with *M. haemolytica* (1×10^5 CFU/mL) for 24 h with or without GOS (24 h) or CLI-095 (1 μM, 3 h) pretreatment. **(A)** The immunoblots were obtained with TLR4, p-p65 and β-actin (protein loading control) (original blots are depicted in Supplementary Fig. S4B). **(B–C)** IL-8 and IL-6 levels in the supernatants of PBECs were measured by ELISA. **(D–G)** PBECs were incubated with LPS (10 μg/mL) or flagellin (10 ng/mL) for 24 h with or without 24 h GOS pretreatment. Levels of IL-8 and IL-6 in the supernatants of PBECs were measured by ELISA. **(H–K)** Human alveolar epithelial (A549) cells and human bronchial epithelial (16HBE) cells were incubated with LPS (10 μg/mL) or flagellin (10 ng/mL) for 24 h with or without 24 h GOS pretreatment. Levels of IL-8 and IL-6 in the supernatants of A549 and 16HBE cells were measured by ELISA. *$P<0.05$; **$P<0.01$; ***$P<0.001$. Data are presented as means ± SEM. All data shown are representative of three independent experiments (n = 3 donor calves or cell generations, one donor calf or one cell generation per experiment).

2.8. Intranasal application of GOS reduces the positivity of *M. haemolytica* in the lungs

Colonization and invasion of *Pasteurellaceae* (e.g., *M. haemolytica*) have been implicated as an important prerequisite for bovine lung infections [22]. Here, the number of *Pasteurellaceae* in the lungs was determined by swabbing BALF on the sheep blood agar plates and counting CFUs [4]. *Pasteurellaceae* in BALF increased significantly over time and peak amount was reached during week 5 (Fig. 8A). Compared with the control calves, the *Pasteurellaceae* CFUs in BALF were significantly lowered by intranasal GOS at week 5 and 7 and maintained at a lower level over time (Fig. 8A).

M. haemolytica-LPS IgG levels were detected in BALF at week 5 (the same timepoint for the measurements of cytokines/chemokines in BALF). The number of control calves positive for *M. haemolytica*-LPS IgG (red dots) was 80% (16/20) at week 5 (Fig. 8B). Interestingly, intranasal GOS significantly lowered the *M. haemolytica*-LPS IgG levels in BALF (Fig. 8B). The detection of *M. haemolytica*-LPS IgG is an indirect method for identifying *M. haemolytica* in BALF. Hence, the positivity for *M. haemolytica* was detected by real-time PCR in BALF at week 5. Fig. 8C showed that 80% (16/20) of control calves were positive for *M. haemolytica*. In line with the data from *M. haemolytica*-LPS IgG detection in BALF (Fig. 8B), this indicates that *M. haemolytica* might be one of the pathogens associated with the lung infection of calves at week

5. Intranasal GOS showed a reduction in the number of calves positive for *M. haemolytica* (50% vs 80%, p = 0.047; Fig. 8C).

Correlations were analyzed to investigate the relation between the CFUs of *Pasteurellaceae* and the levels of *M. haemolytica*-LPS IgG and cytokines in BALF at week 5. Significant positive correlations were observed between the *Pasteurellaceae* CFUs and the *M. haemolytica*-LPS IgG levels in BALF of both control and GOS-spray groups at week 5 (Fig. 8D and E). In addition, positive correlations were observed between the *Pasteurellaceae* CFUs and the IL-6 concentrations in BALF of the GOS-spray group at week 5 (Fig. 8F).

3. Discussion

In this study, we described for the first time that intranasal (local) administration of GOS via spray relieved respiratory inflammation/infection, which might be due to their interesting anti-bacterial, anti-invasive, and anti-inflammatory properties. Airway epithelial cells are the first line of defense against pathogens from invading and infecting lungs [7], and inhibition of bacterial attachment to epithelial cells by carbohydrates has been known for more than three decades [23,24].

As the outbreaks of fatal airway infections by *M. haemolytica* in calves have become increasingly apparent in recent years [2,5], this respiratory pathogen was used for our *in vitro* studies. In the present study, we reported for the first time that GOS inhibited the viability and
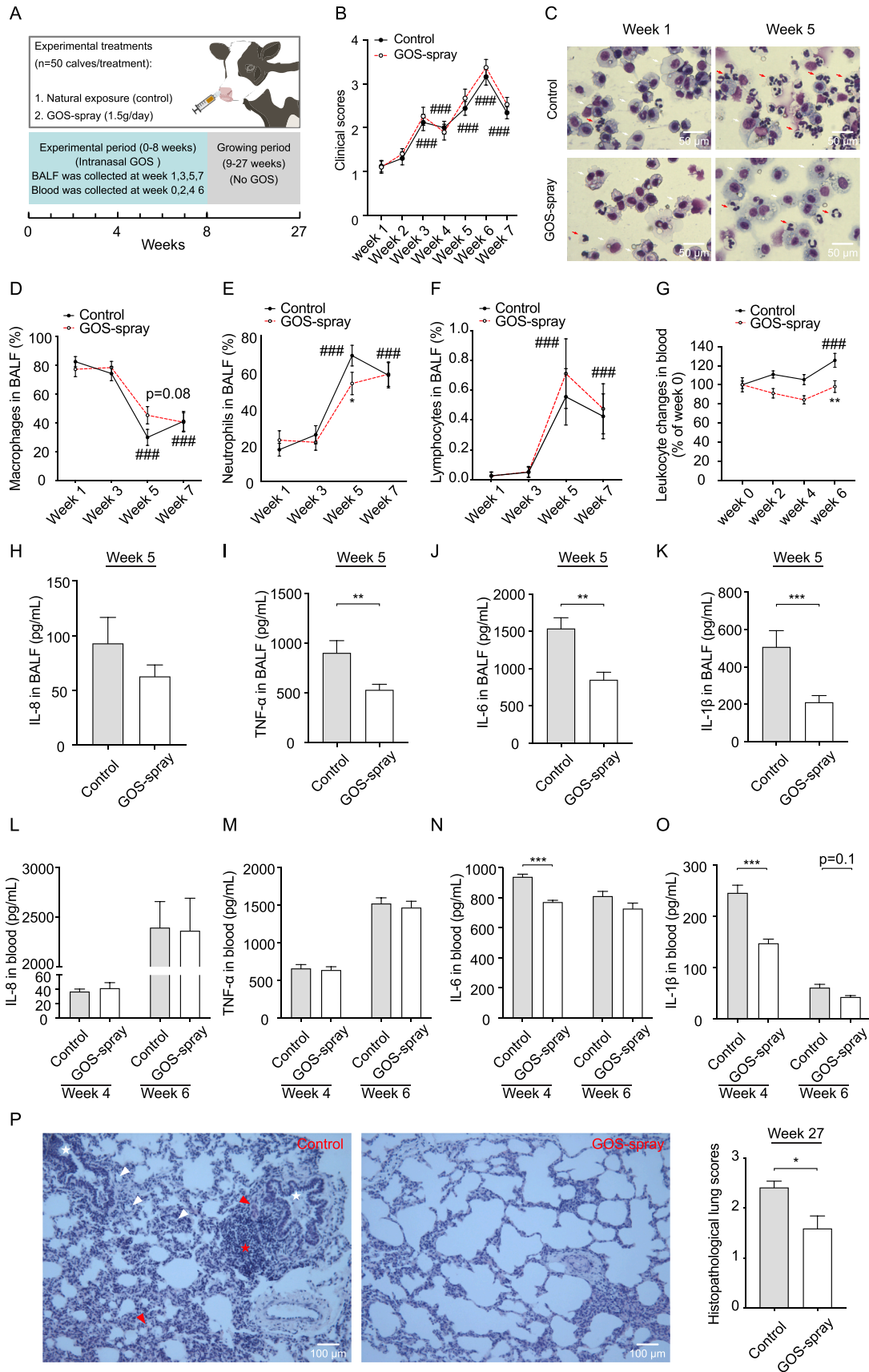
(caption on next page)

Fig. 7. Effect of intranasal GOS on the clinical scores and the cell composition and cytokine/chemokine levels in BALF and blood of calves. (**A**) Timeline and design of the experiment. (**B**) Clinical scores were evaluated over time for all calves (n = 100, 50 calves/treatment). (**C**) Representative cytospins of BALF cell composition including white arrows for macrophages and red arrows for neutrophils. (**D–F**) Percentage of macrophages, neutrophils, and lymphocytes in total BALF cells was determined at week 1, 3, 5 and 7 for a subset of calves (n = 40, 20 calves/treatment). (**G**) Leukocyte changes (vs baseline) in blood were measured at week 0, 2, 4 and 6 for the same subset of calves (n = 40, 20 calves/treatment). (**H–K**) IL-8, TNF-α, IL-6, and IL-1β levels in BALF were measured by ELISA at week 5 for the same subset of calves (n = 40, 20 calves/treatment). (**L–O**) IL-8, TNF-α, IL-6, and IL-1β levels in blood were determined by ELISA at week 4 and 6 for the same subset of calves (n = 40, 20 calves/treatment). (**P**) Right cranial lung lobe of calves in control and GOS-spray groups were collected at week 27. Representative pictures of HE-stained lung sections were depicted. White arrows show collapsed alveoli or thickened alveolar septa; white asterisks outline hyperplasia of bronchus or bronchioles; red asterisk indicates infiltration of inflammatory cells; red arrows show diapedesis of erythrocytes. HE-stained lung sections were scored. Higher histopathological lung scores are related to more lung injury (n = 20, 10 calves/treatment, 10 lung sections/calf). *$P<0.05$; **$P<0.01$; ***$P<0.001$ (GOS-spray vs control at that timepoint); ###$P<0.001$ (control week 3–7 vs week 0 or 1). Data are presented as means ± SEM. (For interpretation of the references to color in this figure legend, the reader is referred to the Web version of this article.)

the growth of *M. haemolytica in vitro*, which may be due to the destruction of the bacterial membranes. The increased membrane permeability by GOS may improve the efficacy of antibiotics against *M. haemolytica*, as 4% GOS lowered the MIC of doxycycline from 0.512 to 0.064 µg/mL and lowered the MIC of oxytetracycline and tilmicosin from 0.512 to 0.032 µg/mL. Interestingly, the additive effect of GOS and doxycycline/oxytetracycline/tilmicosin seemed to be better as compared to the combination with ampicillin. The mechanism of action of β-lactams (e.g., ampicillin) is the interference with bacterial cell wall synthesis, while tetracycline (e.g., doxycycline, oxytetracycline) and macrolide (e.g., tilmicosin) inhibit bacterial protein synthesis by passing through the bacterial membranes, binding to the ribosomal subunit. Due to the interesting additive effect of GOS and antibiotics observed in the MIC assays, the combination of 4% GOS with ampicillin, doxycycline, oxytetracycline, or tilmicosin also showed a promising inhibitory effect on the cytokine/chemokine release in *M. haemolytica*-treated PBECs. Therefore, GOS may act as adjuvants to improve the utility of antibiotics, e.g., in combination with tetracyclines and macrolides. Specific human milk oligosaccharides (HMOs) were able to increase the permeability of the membrane of a Gram-positive coccus, group B Streptococcus (GBS), in a concentration-dependent manner to exert anti-bacterial activity [25]. Moreover, increased membrane permeability also contributed to the improvement of antibiotic efficacy, including gentamicin (aminoglycosides), erythromycin (macrolides) and minocycline (tetracyclines) [26]. HMOs can also increase the efficacy of aminoglycosides (but not of β-lactams) against *Acinetobacter baumannii*, a Gram-negative bacterium [27]. In addition, chitosan oligosaccharide (COS) displayed inhibitory effects on bacterial growth due to increased pore formation and permeabilization of the cell wall of *Bacillus cereus*, whereas the blockage of nutrient flow caused by aggregation of COS is the main reason for the growth inhibition and lysis of *Escherichia coli* [28]. An *in vitro* study showed that the *Actinobacillus actinomycetemcomitans* treated with COS also resulted in the disruption of cell membranes as observed by electron microscopy [29]. Here, lower concentrations of GOS (4%) showed growth inhibition of *M. haemolytica*, while higher concentrations of GOS (8% and 16%) strongly lowered *M. haemolytica* initial viability/CFUs *in vitro*, which may explain the lower bacterial amount, lower *M. haemolytica*-LPS IgG levels, and lower *M. haemolytica* positivity in the lungs of naturally exposed calves treated with intranasal GOS. GOS might reduce proliferation or the number of *M. haemolytica* in the upper respiratory tract, limiting translocation of the pathogen to the lungs. Although more than 4% GOS showed slight toxicity to PBECs after 48 h incubation, the presence of bronchial mucus in calves may dilute the intranasal GOS solution [23]. Moreover, mucociliary clearance, will most probably quickly eliminate intranasal GOS from the airways, as observed in our pilot experiment. In addition, compared with the monolayer model, the calf airways are populated by a diverse microbiota. This commensal microbiota directly inhibits the growth of bacterial pathogens, likely through the competition of available nutrients (e.g., GOS) [30].

In order to cause a lung infection, *M. haemolytica* has developed various strategies for crossing the airway barrier, including adhesion and entry into cells, or simply killing cells to disrupt the airway barrier

[8,21], characterized by destruction of tight and adherens junctions and release of pro-inflammatory cytokines/chemokines by bronchial epithelial cells [8]. To gain more insights into the anti-inflammatory effects of GOS, an *in vitro* infection model using PBECs was established [8]. As expected, the combination of 4% GOS with ampicillin, doxycycline, oxytetracycline or tilmicosin showed better anti-inflammatory properties in *M. haemolytica*-treated PBECs than GOS or the antibiotic alone, which might be mainly due to the higher limitation on the growth of *M. haemolytica*. Interestingly, we observed that lower concentrations of GOS (1% and 2%) can also inhibit the release of IL-8 and IL-6. However, 4% GOS did not show a better anti-inflammatory effect than 2% GOS. This might be partly due to the slight cytotoxic effect of 4% GOS on PBECs, as measured by LDH release after 48 h incubation. In addition, 4% GOS can affect the function of bacterial cell membranes through depolarization. It cannot be excluded that 4% GOS affect the membrane potential of airway epithelial cell membranes or the function of ion channels on cell membranes. Hagenfeld et al. pointed out that hyaluronan (a linear polysaccharide) depolarized the membrane potential of human fibroblasts, human embryonic kidney cells, and central nervous system neurons in a concentration-dependent manner [31]. More research is needed to investigate the effects of GOS on ion channels/transports and membrane potential.

GOS have been reported as anti-adhesives and decoy glycan receptors, which is mainly due to the structural similarity between GOS and various cell surface glycans [10]. For example, GOS competitively inhibit the adhesion of enteropathogenic *E. coli* [32] and *Cronobacter sakazakii* [33] to host epithelial cells and the binding of *Vibrio cholerae* toxin to the toxin receptor (GM-1) of host cells [34]. In the present study, although 2% GOS did not have the ability to inhibit the growth of *M. haemolytica*, it might act as a decoy glycan to competitively bind to the carbohydrate moiety on bronchial epithelial cells, preventing the invasion and adhesion of *M. haemolytica*.

GOS prevented the TEER decrease and altered expression of tight and adherens junction-related proteins (ZO-1 and E-cadherin) induced by *M. haemolytica*, maintaining the functional airway epithelial barrier integrity. On one hand, the inhibition of 2% GOS on the adhesion to and invasion of PBECs by *M. haemolytica* might prevent the subsequent release of inflammatory mediators, such as cytokines/chemokines and the disruption of the airway epithelial barrier (Fig. 8G). On the other hand, GOS might eliminate the adverse effects of the released endotoxins (e.g., LPS) and exotoxins (e.g., leukotoxin) (from *M. haemolytica*) on bronchial epithelial cells, due to their ability to interfere or neutralize bacterial toxins [10]. Although in our study undifferentiated PBECs were used, the liquid-liquid system does not force the maturation and ciliation of epithelial cells and can retain some epithelial progenitor cells and non-ciliated cells, which are also present/play an important role in the airways in health and disease [35,36]. In addition, our *ex vivo* model can create an intact airway epithelial barrier with well-developed junctional complexes and exhibit an inflammatory response after stimulation with *M. haemolytica* and other stimulants (LPS and flagellin).

Remarkably, 2% GOS inhibited the invasion of and adhesion to PBECs by *M. haemolytica* without affecting the bacterial growth in the supernatants. This might be due to the small amount (0.6×10^5 CFU/
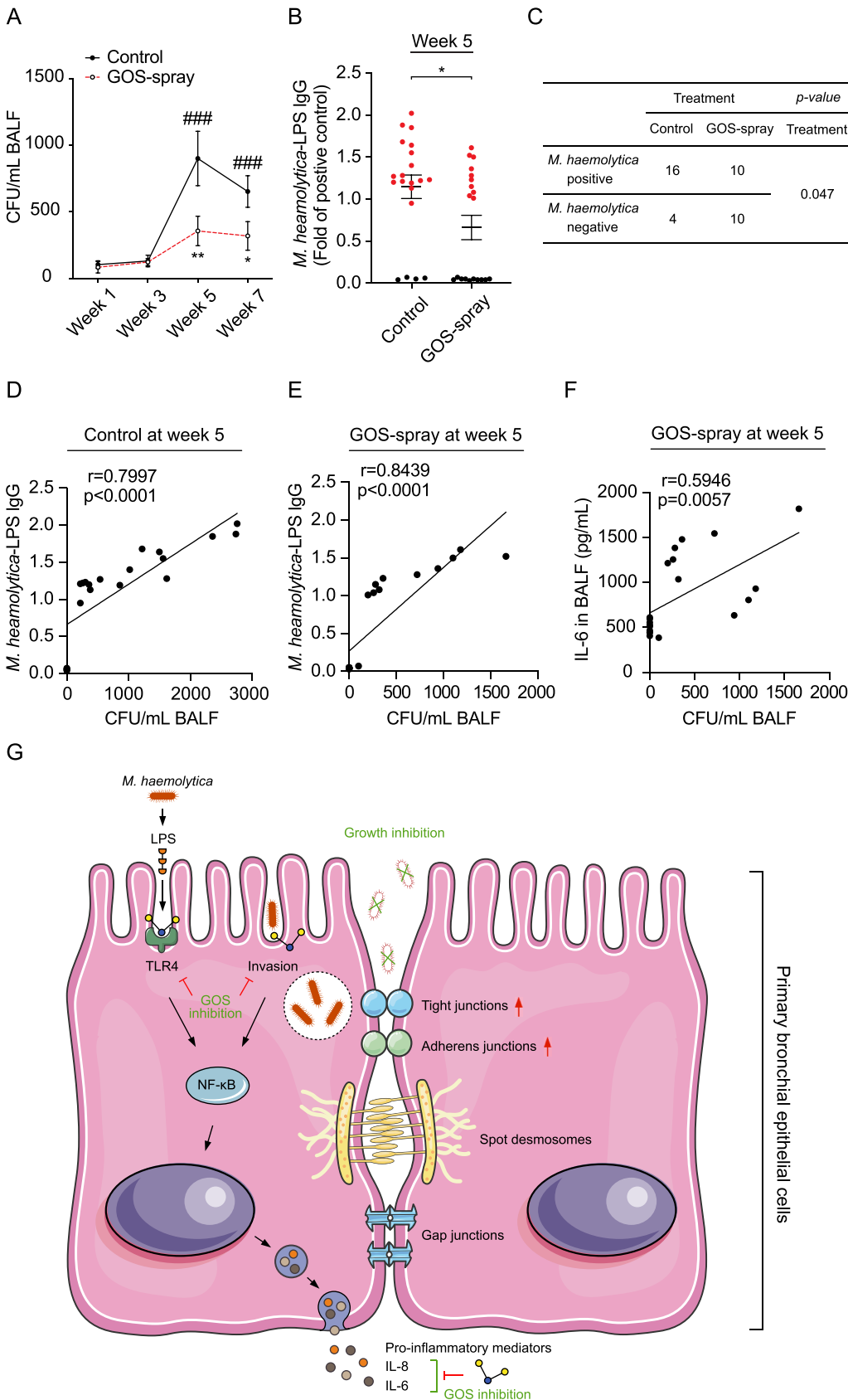
Fig. 8. Intranasal GOS reduce the positivity of *M. haemolytica* in the lungs. (A) BALF was inoculated onto the 5% sheep blood agar plates and CFUs of *Pasteurellaceae* were counted over time for the same subset of calves (n = 40, 20 calves/treatment). (B) *M. haemolytica*-LPS lgG levels was detected in BALF from the same subset of calves at week 5 by ELISA (n = 40, 20 calves/treatment). Compared to the positive control, fold changes were calculated. Black dots represent *M. haemolytica*-LPS lgG negative calves. Red dots represent *M. haemolytica*-LPS lgG positive calves. (C) Number of *M. haemolytica* positive and negative calves according to the presence in BALF by real-time PCR method. (D–E) Correlations between the CFUs of *Pasteurellaceae* and the levels of *M. haemolytica*-LPS lgG in BALF of control and GOS-spray treatment groups at week 5. (F) Correlations between the CFUs of *Pasteurellaceae* and the concentrations of IL-6 in BALF of GOS-spray treatment group at week 5. *P<0.05; **P<0.01 (GOS-spray vs control at that timepoint); ###P<0.001 (control week 5 or 7 vs week 1). Data are presented as means ± SEM. (G) A postulated underlying mechanism for GOS to protect the bronchial epithelial cells from *M. haemolytica*-induced infection and subsequent inflammation. On the one hand, GOS may lower *M. haemolytica* viability by damaging the bacterial cell membrane. On the other hand, GOS is thought to act as a soluble decoy receptor, resulting in reduced adhesion to and invasion of airway epithelial cells by *M. haemolytica*. This inhibits the release of cytokines/chemokines and prevents *M. haemolytica* from entering the cells through endocytosis and damaging the airway barrier integrity. In addition, GOS can also inhibit the release of cytokines/chemokines induced by one of the virulence factors of *M. haemolytica*, LPS, thereby protecting the impairment of airway epithelium caused by the accumulation of inflammatory mediators. (For interpretation of the references to color in this figure legend, the reader is referred to the Web version of this article.)

mL) of *M. haemolytica* that invades PBECs, while a significant amount $(0.9 \times 10^8 \text{ CFU/mL})$ is exponentially growing in the supernatant and affecting PBECs by releasing virulence factors (e.g., LPS). *M. haemolytica*-derived LPS has the ability to induce airway epithelial inflammation and barrier dysfunction, possibly through the recognition of TLRs [2,8]. In our study, the TLR4 protein expression and downstream p-p65 were increased in PBECs after *M. haemolytica* exposure, indicating activation of TLR4/NF-κB pathway, resulting in the induction of IL-8 and IL-6 [37]. Furthermore, the TLR4 inhibitor, CLI-095, lowered the TLR4 protein expression, the NF-κB p65 phosphorylation, and the release of IL-8 and IL-6 in PBECs after *M. haemolytica* exposure, suggesting a potential role for TLR4 in the *M. haemolytica*-induced inflammation [37]. However, CLI-095 cannot prevent the *M. haemolytica*-induced disruption of the PBEC monolayer integrity. This might be explained by the ability of *M. haemolytica* to destroy the epithelial barrier mainly through adhesion, invasion, and explosive replication [21] instead of activation of TLR4. Interestingly, GOS (2%) not only prevented the adhesion and invasion of *M. haemolytica* to PBECs but also inhibited the *M. haemolytica*-induced activation of the TLR4/NF-κB pathway (Fig. 8G). This might be the reason that although both GOS and CLI-095 inhibit TLR4/NF-κB pathway, the anti-inflammatory effect of GOS seems to be more pronounced than observed with CLI-095. In addition, GOS also decreased the LPS- but not flagellin-induced epithelial inflammation in both human and bovine airway epithelial cells. Although these results provide indirect evidence, it can be suggested that GOS might specifically inhibit the recognition of LPS by TLR4. Increasing evidence showed that NDOs are directly or indirectly involved in the TLR4/NF-kB pathway [10,38,39]. For example, HMOs (2′-fucosyllactose and 6′-sialyllactose) were reported to inhibit TLR4 expression and signaling in mouse and piglet necrotizing colitis models and human (infant) intestinal explants, probably due to the capacity of HMOs to directly dock into the LPS-binding pocket of TLR4 [40].

Our previous study has demonstrated that oral GOS can exhibit anti-inflammatory effects and relieve lung infections in calves, which might be due to the inhibition of NLRP3 inflammasome activation [41]. Here, intranasal GOS were innovatively applied to calves with naturally occurring lung infections due to the anti-bacterial and anti-invasive effects of GOS described *in vitro*. Breastfeeding infants ingest mother milk several times per day, bathing the nasopharynx for several minutes at each feeding with a solution high in HMOs, which might inhibit local bacterial adherence [24]. *In vivo,* it has been observed that oral supplemented GOS and/or FOS can also have beneficial effects on the airways [42–44]. The present study showed that intranasal GOS partly reduced local and systematic inflammation, indicated by a decreased concentrations of TNF-α, IL-6 and IL-1β in BALF and IL-6 and IL-1β in blood. Although the total cell numbers (mainly pulmonary leukocytes) in BALF did not reduce in the GOS-spray group, intranasal GOS restored markedly the ratios of macrophages to neutrophils, as indicated by more macrophages and fewer neutrophils, which is commonly observed in the lower respiratory tract of healthy calves [45,46]. Neutrophils can be recruited and activated by multiple pro-inflammatory mediators including IL-8, TNF-α, IL-6 and IL-1β [47,48], while excessive accumulation of neutrophils and pro-inflammatory mediators can mediate tissue damage in the lungs [49]. After 27 weeks of natural exposure, HE-stained lung tissue of calves showed indications of lung injury, including collapsed alveoli or thickened alveolar septa, hyperplasia of bronchus or bronchioles, infiltration of inflammatory cells, and/or diapedesis of erythrocytes. Calves receiving intranasal GOS administration exhibited lower histopathological lung scores compared to control calves, highlighting the importance of early NDO intervention to prevent lung infections.

GOS also prevented the increase of leukocytes in blood. The differences between control and GOS-spray treatments were more obvious in parameters measured in BALF compared to blood, which might be related to the local GOS administration and possible rapid removal from

the distal trachea by mucociliary clearance [23,50]. Furthermore, it cannot be excluded that part of the effects of GOS might be related to spillover in the esophagus. In addition, the anti-inflammatory and immunomodulatory effects of GOS that occurred during experimental week 5 and seemed to disappear during week 7, might be related to (1) the group antibiotic treatments for all calves based on clinical scores at week 6 and/or (2) the innate immune system activation (increased BALF neutrophils and blood leukocytes) during week 5/6, which contributes to partly eliminating/phagocytosing the pathogens in the lungs. In the future, investigating the effect of intranasal application of GOS in combination with antibiotics (e.g., tetracyclines and/or macrolides) on the treatment of lung infections might be interesting.

GOS have already been approved as a safe food additive in infant formula in Europe, USA and China [51–54]. The maximum daily intake in the general population recommended by European Food Safety Authority (EFSA) would be no more than 16.2 g GOS [54]. A safety study of GOS in rats demonstrated that a maximum daily intake of 2 g/kg was safe [55]. While the daily intake of GOS in the present calf study was approximately 0.03 g/kg (1.5 g/day/calf, the average calf was 43.3 kg at the start of the experiment), which is far below the maximum recommended daily (oral) intake. The dosage of 15% GOS (1.5 g GOS/10 ml saline) was used according to the promising anti-pathogenic effects of 8% and 16% GOS *in vitro*. In addition, 1.5 g GOS/10 ml saline can be properly atomized by spray and can reach the lower respiratory tract as observed in our pilot calf study, while higher concentrations of GOS (>1.5 g GOS/10 ml saline) showed a poor atomization efficiency. After the nasal GOS spray, GOS will probably be gradually distributed by gravity and respiration and serially diluted by the action of the mucociliary system in the epithelial lining fluid of the respiratory tract [23]. However, the biosafety of intranasal administration of GOS is not available and warrants more research.

Although our group and Logtenberg et al. have worked on the measurement of GOS structures via chromatography and mass spectrometry, respectively [16,17], the exact chemical structure of GOS is still not fully understood due to the continuous discovery of new isomers. Moreover, van Leeuwen et al., Logtenberg et al. and Akbari et al. measured the percentages of galactose, glucose and GOS DP2-6 in Vivinal GOS (the same GOS as used in the present study) via size-exclusion chromatography [16–18]. Different GOS DPs exhibit differential biological properties. Ladirat et al. indicated that GOS DP ≥ 4 was more efficient than GOS DP ≤ 3 in restoring *Bifidobacterium* levels in antibiotic-disrupted microbiota from adults [56]. In addition, Sinclair et al. showed that higher DP of GOS could inhibit the *in vitro* binding of *Vibrio cholerae* toxin to its cell-surface toxin (GM1) receptor [34]. Our previous study showed that barrier protective effects of GOS were related to the GOS structures, because DP2 and DP3 exhibited a higher protective effect on the intestinal barrier integrity than higher DPs in a Caco-2 cell model for intestinal barrier dysfunction. In contrast, GOS DP6 showed more promising anti-inflammatory effects than lower DPs [17]. However, to date, there is no evidence of the exact relationship between the structure of individual GOS components and their anti-bacterial effects. Therefore, we should investigate the effect of different GOS DPs on *M. Haemolytica* in the future.

Our study showed that local administration of GOS suppressed the *Pasteurellaceae* numbers in BALF. It has been described that inoculation of BALF on sheep blood agar is a fast and economical method for screening *Pasteurellaceae* (*M. haemolytica, P. multocida* and *H. somni*) with usually pure cultures, high isolation rates and less nasopharyngeal contamination [4,57,58]. However, with this assay we cannot distinguish between *M. haemolytica* and other *Pasteurellaceae* (*P. multocida* and *H. somni*) on sheep blood agar. Therefore, *M. haemolytica*-LPS lgG detection and real-time PCR were used to confirm the positivity for *M. haemolytica* in BALF/lungs. Up to 80% of control calves were positive for *M. haemolytica* in BALF at week 5, indicating that *M. haemolytica* might be one of the pathogens involved in the lung infections of the present study. Interestingly, intranasal GOS reduced the

M. haemolytica-LPS lgG levels *and M. haemolytica* positivity in BAL-F/lungs. Furthermore, positive correlations were observed between the *Pasteurellaceae* CFUs and *M. haemolytica*-LPS lgG levels in BALF of control and intranasal GOS treatments, indicating probably a reduced number of *M. haemolytica* existed in the lower respiratory tract of calves treated with intranasal GOS, which might be due to the anti-bacterial and anti-invasive effects of GOS observed *in vitro*. In addition, the suppressed *Pasteurellaceae* (possibly *M. haemolytica*) number in BALF caused by intranasal GOS may contribute to the reduced cytokine concentrations and neutrophil numbers in BALF. The release of *M. haemolytica*-LPS is one of the causes of airway inflammation observed in lung infections [6,22]. The decreased airway inflammation in infections might be related to the specific inhibition of LPS-induced inflammation by GOS.

In addition, possible GOS-induced changes in the nasal commensal bacteria may contribute to the *M. haemolytica* inhibition in BALF. GOS intervention has been widely used to stimulate the growth of *Bifidobacterium* and/or *Lactobacillus* species in the gut [10]. A recent study in calves showed that intranasal administration of *Lactobacillus* strains reduces the nasal colonization of *M. haemolytica*, which might be due to the competition for adherence to the mucosa or direct growth inhibition [58].

Single-pathogen challenge models experimentally inoculate a large number of pathogenic bacteria (e.g., *M. haemolytica*) in the lower respiratory tract [58,59], however, ignore the complexity of the naturally acquired infection, involving the invasion of opportunistic bacteria caused by stress, weakened immunity, environmental factors, close contact transmission, etc. [6]. In order to prevent high mortality, antibiotic strategies have been applied for all calves in the present study, which may reduce the observed clinical scores and postpone the occurrence of lung infections. During week 5 of our naturally exposed calves, the clinical score increased by 1.5-fold, macrophages decreased extensively, lymphocytes increased slightly, while neutrophils increased expansively (11-fold) in BALF and were the predominant cell type in BALF, indicating that lung infections, most probably bacterial infections [46,57], are present from week 5. Therefore, chemokine/cytokine parameters in BALF were mainly measured at week 5. In addition, the peak number of *Pasteurellaceae* in BALF also supports our conclusion that a bacterial outbreak was present in the lungs during week 5. Blood parameters were measured one week prior to or one week after BALF collection, to minimize the disadvantages of invasive measurements of both BALF and blood collection during the same week [6]. However, in naturally occurring or experimentally inoculated lung infections, clinically healthy or asymptomatic individuals might be present [4,58]. This could be the reason why the effect of GOS spray on BALF composition and clinical scores might be underestimated. In addition, the insensitivity of clinical scores to the diagnosis of (subclinical) lung infections may also lead to contrasting results as compared to the measurements of cell composition and cytokine/chemokine levels in BALF/blood [57].

4. Conclusions

In summary, it can be concluded that high concentrations of GOS (8% and 16%) significantly reduced the viability of *M. haemolytica in vitro*. Next to that, 4% GOS lowered the growth of *M. haemolytica* and enhanced the efficacy of antibiotics, especially macrolide and tetracycline, against *M. haemolytica*. In addition, 2% GOS prevented *M. haemolytica* from adhering to and invading of PBECs and inhibited the activation of the "TLR4/NF-κB" pathway, which contributed to a reduced cytokine/chemokine release and restored airway epithelial barrier. Although GOS had no effect on clinical scores, the intranasal administration of GOS relieved the inflammatory response and reduced the *M. haemolytica* positivity during naturally occurring lung infections. Therefore, this study proposes a promising new strategy for the clinical evaluation of local application of GOS in other animals and humans (children) suffering from respiratory infections.

5. Materials and methods

5.1. M. haemolytica growth and bacteriostatic assay

M. haemolytica isolated from a pneumonic calf lung was cultured on agar plate enriched with 5% sheep blood (bioTRADING, Mijdrecht, The Netherlands) at 37 °C as previously described [8].

Subsequently, *M. haemolytica* (1×10^5 CFU/mL) was collected from the blood agar plate and incubated in 96-well plates with or without different concentrations of GOS (0.25%–16%; Vivinal GOS syrup, FrieslandCampina Ingredients, Amersfoort, The Netherlands), ampicillin (0.001–1.024 μg/mL; Sigma-Aldrich, Zwijndrecht, The Netherlands), doxycycline (0.001–1.024 μg/mL; Sigma-Aldrich), oxytetracycline (0.001–1.024 μg/mL; Sigma-Aldrich), tilmicosin (0.001–1.024 μg/mL; Sigma-Aldrich), GOS + ampicillin (2% or 4% + 0.002–0.016 μg/mL), GOS + doxycycline (2% or 4% + 0.016–0.256 μg/mL), GOS + oxytetracycline (2% or 4% + 0.016–0.256 μg/mL), or GOS + tilmicosin (2% or 4% + 0.016–0.256 μg/mL) for 24 h. After incubation, *M. haemolytica* growth was determined by measuring the turbidity of supernatants at OD600nm using a microplate reader (Promega Corp., Madison, WI) and presented as OD values. The MIC of GOS, antibiotics, GOS + antibiotics were recorded as the lowest concentration at which no bacterial growth was observed.

5.2. Bactericidal assay

M. haemolytica (1×10^5 CFU/mL) was cultured in 96-well plates with or without GOS (4%, 8%, and 16%) treatments for 24 h. Then, the supernatants were diluted and sub-cultured onto 5% sheep blood agar plates (bioTRADING) overnight at 37 °C. *M. haemolytica* CFUs on each agar plate were counted and calculated as CFU/mL based on the dilution factor of 50,000 for *M. haemolytica* group and 4% GOS treatment and dilution factor 100 for 8% and 16% treatments.

M. haemolytica (1×10^5 CFU/mL) was diluted and sub-cultured overnight onto 5% sheep blood agar plates (bioTRADING), which were precoated with 5 mL 4%, 8% or 16% GOS via swabbing. *M. haemolytica* numbers were determined by counting *M. haemolytica* CFUs on each agar plate and calculated as CFU/mL based on the dilution factor of 100.

5.3. Bacterial live/dead and membrane potential assay

LIVE/DEAD BacLight assay (Invitrogen, ThermoFisher Scientific, Waltham, MA) was applied to assess the live/dead ratios and bacterial membrane integrity according to manufacturer's instructions. Briefly, *M. haemolytica* (1×10^5 CFU/mL) was cultured in 96-well plates with or without GOS (0.5%–16%) treatments for 24 h and stained with PI and SYTO 9 dye for 15 min prior to evaluation with a fluorometer (Promega Corp.) at excitation/emission 485/530 nm (green, SYTO 9) and 485/630 nm (red, PI). The live/dead ratio was calculated as a ratio of green to red fluorescence (ratio = green/red).

M. haemolytica (1×10^5 CFU/mL) was cultured in 96-well plates with or without 2% or 4% GOS treatments for 24 h and stained with PI and SYTO 9 dye for 15 min. After staining, 5 μL bacterial suspension was pipetted onto a glass slide and determined for the bacterial membrane integrity by a microscope (Keyence BZ-9000, KEYENCE Corporation, Itasca, IL). SYTO 9 is a dye that passes through intact membranes to stain live bacteria green, while PI is a larger molecular dye that can only pass through membranes that have lost integrity to stain dead bacteria red [25]. The number of live (green) and dead (red) *M. haemolytica* was counted by Image J 1.8.0, (National Institutes of Health, Bethesda, MD) and presented as the proportion of *M. haemolytica* with damaged membrane.

The membrane potential of *M. haemolytica* after treatments was measured by the BacLight bacterial membrane potential kit (Invitrogen, Thermo Fischer Scientific) following the manufacturer's instruction.

Briefly, *M. haemolytica* (1×10^5 CFU/mL) was cultured in 96-well plates with or without 2% or 4% GOS treatments for 12 or 24 h and normalized by optical density at a wavelength of 600 nm. After normalization, CCCP (5 μM) was added to one of the untreated bacterial suspensions as the depolarized control (positive control). Thereafter, all conditions were incubated with $DiOC_2(3)$ (30 μM) at room temperature for 30 min. Fluorescence was measured using a fluorometer (Promega Corp.) at excitation/emission 485/530 nm (green) and 485/630 nm (red). The ratio parameter (red/green fluorescence ratio) allows for the measurement of bacterial membrane potential.

5.4. Isolation and culture of PBECs

Isolation and culture of PBECs were conducted as previously described [8]. Briefly, PBECs were isolated from bovine bronchial epithelium obtained from the lungs of freshly slaughtered calves aged 6–8 months provided by Ekro bv (Apeldoorn, The Netherlands). After digesting of the bronchial epithelium, PBECs were collected and grown in 5% CO_2 at 37 °C and attached to collagen-coated plates in serum-free RPMI-1640 medium [8] for 2–3 days until reaching near-confluence. After that, PBECs were washed 3 times with warm PBS (Sigma-Aldrich) and replaced with RPMI-1640 medium (Lonza, Verviers, Belgium) containing 10% FBS (Sigma-Aldrich), 1% L-glutamine, and 1% MEM NEAA (Gibco, Thermo Fisher Scientific) for cell culture and experiments.

5.5. Human airway epithelial cell line culture

Human Type II alveolar epithelial cells (A549; ATCC, Manassas, VA) were grown in Ham's F–12 K Medium (Gibco) supplemented with 10% FBS and 1% penicillin-streptomycin (Gibco) in 5% CO_2 at 37 °C. Human bronchial epithelial cells (16HBE; Sigma-Aldrich) were grown in MEM (Gibco) supplemented with 10% FBS, 1% L-glutamine and 1% penicillin–streptomycin in 5% CO2 at 37 °C.

5.6. Cell treatments

PBECs were cultured at a density of 1×10^6 cells/mL in collagen precoated 96- and 6-well plates as previously described [8]. After reaching near-confluence, PBECs were pretreated with or without GOS (4%), ampicillin (0.016 μg/mL), doxycycline (0.032–0.256 μg/mL), oxytetracycline (0.016–0.032 μg/mL), tilmicosin (0.016–0.032 μg/mL), GOS + ampicillin (4% + 0.016 μg/mL), GOS + doxycycline (4% + 0.032–0.256 μg/mL), GOS + oxytetracycline (4% + 0.016–0.032 μg/mL), or GOS + tilmicosin (4% + 0.016–0.032 μg/mL) for 24 h prior to 24 h *M. haemolytica* (1×10^5 CFU/mL) exposure.

To measure the cytotoxicity (LDH and MTT assays) of GOS, PBECs were treated with or without increasing concentrations of GOS (0.25%–16%) for 48 h. In addition, to investigate the anti-inflammatory or anti-invasive properties of GOS, PBECs were pretreated with or without lower concentrations of GOS (0.5%–2%) for 24 h or CLI-095 (1 μM; TLR4 inhibitor, Invivogen, San Diego, CA) for 3 h prior to 24 h *M. haemolytica* (1×10^5 CFU/mL), 24 h LPS (10 μg/mL; isolated from *E. coli* O111:B4, Sigma-Aldrich) or 24 h flagellin (10 ng/mL; isolated from *P. aeruginosa*, Invivogen) exposure. After exposure, PBECs were harvested, and supernatants were collected and stored at −20 °C until analysis.

A549 or 16HBE cells were cultured at a density of 0.5×10^5 cells/mL in 96-well plates. After reaching near-confluence, A549 or 16HBE cells were pretreated with 1% or 2% GOS for 24 h prior to 24 h LPS (10 μg/mL; Sigma-Aldrich) or flagellin (10 ng/mL; Invivogen) exposure. After exposure, supernatants were collected and stored at −20 °C until analysis.

5.7. Bacterial invasion and adhesion assay

PBECs (1×10^6 cells/mL) were grown in 6-well plates. After different treatments, the absorbance of supernatants was measured at 600 nm using a microplate reader (Promega Corp.), thereafter the supernatants were diluted and sub-cultured onto 5% sheep blood agar plate overnight at 37 °C. *M. haemolytica* growth in the supernatants was presented as OD values. *M. haemolytica* numbers in the supernatants were determined by counting *M. haemolytica* CFUs on each agar plate and calculated as CFU/mL based on the dilution factor of 50,000.

To quantify the number of invaded bacteria, extracellular *M. haemolytica* was killed by adding fresh medium containing 250 μg/mL gentamicin (Sigma-Aldrich) to PBECs for 3 h incubation. PBECs were rinsed three times with warm PBS and lysed by 1% Triton X-100 (Sigma-Aldrich). The suspensions were collected, diluted, and sub-cultured onto 5% sheep blood agar plate overnight at 37 °C. *M. haemolytica* numbers were determined by counting *M. haemolytica* CFUs on each agar plate and calculated as CFU/mL based on the dilution factor of 1000.

To calculate the number of adherent bacteria, PBECs were rinsed three times with warm PBS to remove non-adherent *M. haemolytica* and lysed by 1% Triton X-100. The suspensions were collected, diluted, and sub-cultured onto 5% sheep blood agar overnight at 37 °C. *M. haemolytica* numbers were determined by counting *M. haemolytica* CFUs on each agar plate and calculated as CFU/mL based on the dilution factor of 1000. Adherent bacteria were calculated as: [the number of total bacteria] – [the number of invaded bacteria].

5.8. TEER measurement and paracellular tracer flux assay

PBECs (1×10^6 cells/mL, 300 μL) were added to the apical compartment of the permeable 0.3 cm^2 high pore density polyethylene membrane transwell inserts placed in a 24-well plate (Corning). After that, 700 μL cell culture medium was added to the basolateral compartment, prior to incubation in 5% CO_2 at 37 °C. TEER of PBECs was measured by a Millicell-ERS Volt-Ohm meter (Millipore, Merck, Darmstadt, Germany) every 2 days. The culture medium from the apical and basolateral compartment was refreshed after TEER measurement and experiments started at day 11 when sustained TEER values around 600 Ω cm^2 were reached as described before [8].

PBECs were exposed to *M. haemolytica* (1×10^5 CFU/mL) from the apical side with or without 24 h GOS pretreatment or 3 h CLI-095 pretreatment at both the apical and basolateral compartments. TEER was measured at 0 h and 24 h after *M. haemolytica* exposure. Thereafter, a membrane-impermeable molecule, lucifer yellow (molecular mass of 0.457 kDa, 20 μg/mL; Sigma-Aldrich), was added to the apical compartment for 4 h, and the paracellular flux was determined by measuring the fluorescence intensity at the basolateral compartment with a fluorometer (Promega Corp.) set at excitation/emission wavelengths of 410/520 nm. After measurement, PBECs were harvested for immunofluorescence staining and western blotting, and supernatants were collected and stored at −20 °C until analysis.

5.9. Thiazolyl blue tetrazolium bromide (MTT) and LDH assay

After different treatments, the viability of PBECs was measured using MTT assay. MTT (Sigma-Aldrich) was dissolved at a final concentration of 0.5 mg/mL in cell culture medium. Each culture well was delicately washed with warm PBS before adding a 120 μL MTT solution. After 3 h of incubation (37 °C, 5% CO_2), the formed formazan crystals were dissolved in 100 μL of dimethyl sulfoxide (Sigma-Aldrich) and absorbance was read at 595 nm using a microplate reader (Bio-Rad Laboratories, Hercules, CA).

LDH was measured in the supernatants of PBECs after different treatments using the CytoTox 96 nonradioactive cytotoxicity assay kit (Promega Corp.) according to manufacturer's instructions.

5.10. Western blotting

Western blotting of cell lysates after different treatments and the information of primary/secondary antibodies were described previously [8]. Digital images were acquired with the Molecular Imager (Gel DocTM XR, Bio-Rad Laboratories) and analyzed with Image lab 5.0 (Bio-Rad Laboratories).

5.11. Immunofluorescence

The tight junction ZO-1 and the adherens junction protein E-cadherin of PBECs were detected using immunofluorescence microscopy as previously described [8]. ZO-1 and E-cadherin were visualized, and images were taken using the Keyence BZ-9000 (KEYENCE Corporation). Fluorescence intensity was quantified by Image J 1.8.0 and presented as fluorescence intensity (vs DAPI).

5.12. Animals and experimental design

The animal experiment was conducted at the research facilities of the VanDrie Group (Scherpenzeel, The Netherlands) and was approved by the Animal Care and Use Committee of Wageningen University (AVD1040020185828, Wageningen, The Netherlands).

One hundred male Holstein-Friesian calves 18 d of age (43.3 ± 0.32 kg, means ± SEM) of German origin were used and assigned randomly to 2 treatments. The control treatment included 50 calves. The GOS-spray treatment included 50 calves that received intranasal GOS (1.5 g GOS/ 10 mL saline). GOS were dissolved in warm saline and sprayed into the nasopharynx through an intranasal applicator (Rispoval, Zoetis B.V., The Netherlands) mounted on the top of the 10 mL syringe. The GOS-spray treatment received intranasal GOS from experimental week 1–8, while no GOS was applied from week 9–27. During the experimental week 0–8, clinical scores were weekly assessed for all calves (50 calves/ treatment), while cytokine/chemokine concentrations and leukocyte parameters in blood and BALF were analyzed bi-weekly for a subset of calves (20 calves/treatment) unless otherwise indicated. The subset of calves included 2 calves per pen, resulting in 20 calves per treatment. Per pen, the 2 calves whose arrival body weight was closest to the mean body weight of all calves at arrival, were included in this subset.

During the whole experiment, all calves were naturally exposed to pathogens in the environment (natural incidence of disease, animals were not challenged). Individual antibiotic treatment was applied when required based on clinical signs of illness as assessed by the animal caretakers. The number of applied individual antibiotic treatments did not differ between the control and GOS-spray groups ($P > 0.1$). Group antibiotic treatment was applied equally to all groups if 10% of the calves had been treated within 5 days, or if 5% of the calves had become ill within 24 h or when the situation required group antibiotics in the expert judgement of a veterinarian.

The *in vivo* study described in this article is part of a large calf trial, including 300 calves randomly assigned to a control treatment, a GOS-spray treatment and four treatments with different dietary interventions (50 calves/treatment) [41]. In accordance with the purpose of this study, investigating the effect of intranasal GOS on lung infections, we reported here the results of the analyses of the control and GOS-spray treatments (100 of 300 calves) of this large calf trial.

5.13. Housing and feeding

Calves were housed in a mechanically ventilated indoor stable throughout the experiment. The climate guidelines included that, in the first 3 weeks, a minimum temperature of 15 °C was maintained and heat canons were used when needed. Thereafter, ventilation rates are adjusted to maintain a maximum ΔT of 5 °C compared to the outside temperature and a maximum relative humidity of 80%. The ambient lighting consisted of natural lighting plus artificial lighting from 0600 to 1800 h. Calves were housed in pens (9 m²) containing wooden-slatted floors. In the first 6 weeks after arrival, individual housing was applied (1.2 m²/calf) by placing stainless steel fences within the pens. After 6 weeks, the individual fencing was removed, and calves were housed in groups of 5.

All calves were fed with milk replacer (MR) twice a day. The MR mainly contained 527 g/kg whey powder, 35 g/kg lactose, 52 g/kg delactosed whey powder, 50 g/kg whey protein concentrate, 60 g/kg soy protein concentrate, 50 g/kg soluble wheat protein, 3 g/kg pea fiber, 179.4 g/kg fat sources, 9.7 g/kg calcium formate, 2 g/kg citric acid, 4 g/ kg sodium bicarbonate, 3.5 g/kg mono ammonium phosphate, 9.8 g/kg lysine, 2.4 g/kg methionine, 1.3 g/kg threonine, 0.2 g/kg aroma (LUCTAROM L, Lucta, Barcelona, Spain) and 10 g/kg premix. In addition to the MR, all calves received the same solid feed starting 1 week after arrival [44].

5.14. Clinical scores

Clinical scoring was performed weekly for all calves, adapting from the Wisconsin calf respiratory scoring system [60], in which a score from 0 to 3 was provided for rectal temperature, coughing, nasal discharge and behavior. Clinical score was calculated as the sum of these 4 scores. The higher the clinical score, the more severe respiratory diseases.

5.15. Blood sampling and hematological analysis

Blood samples were collected in all calves by venipuncture in the jugular vein at arrival before the first MR feeding (baseline, week 0), and then were collected repeatedly in the subset of calves at experimental week 2, 4 and 6. Blood was collected in K_2-EDTA tubes and was kept on ice for collection of plasma or kept at room temperature for analysis of leukocyte numbers the same day by fluorescence flow cytometry using a Sysmex 1800iV (Sysmex Europe GmbH, Norderstedt, Germany). Plasma was collected after centrifugation at 2000×g and 4 °C for 20 min and was stored at −20 °C pending further cytokine/chemokine measurement by ELISA.

5.16. BALF sampling and phenotyping

BALF samples were collected repeatedly for the same subset of calves (20 calves/treatment) at experimental week 1, 3, 5 and 7 and obtained by use of a technique adapted from a previous description [61]. Once wedged the sterilized 100 cm BAL catheter in the appropriate location of the lungs, a syringe was connected to the catheter and a total of 30 mL of sterile saline (37 °C) solution was infused into the tube and fluid was immediately aspirated from the bronchus. BALF (18.5 ± 0.39 mL, means ± SEM) was obtained from each calf and was stored in a 50 mL tube on ice until further analysis the same day.

BALF suspension was filtered by passing through a 70 μm cell strainer (Corning) to remove debris. Then, BALF suspension was centrifuged (400×g, 4 °C for 5 min) and the remaining cell pellet was resuspended in 1 mL cold FBS. After centrifugation, the supernatant was aliquoted into 1.5 mL tubes and stored at −80 °C for further analysis. The number of the remaining cell pellet was determined by automatically counting using a Cellometer Bright Field cell counter (Nexcelom Bioscience, Lawrence, MA). After counting, 0.5×10^6 cells of BALF were used to make cytospins stained with Diff-Quick (Medion Diagnostics International Inc., Miami, FL) and a minimum of 400 cells were counted. Phenotyping was determined by a microscope (Olympus BX50, Olympus Life Science, Tokyo, Japan).

5.17. Quantifying the number of Pasteurellaceae in BALF

BALF was collected and stored as described above. Thereafter, 50 μL BALF was inoculated onto blood agar enriched with 5% sheep blood (bioTRADING) for isolation of *Pasteurellaceae* and incubated overnight

at 37 °C as described before [4]. The identification of *Pasteurellaceae* was based on morphological characteristics [58,62] and the number of *Pasteurellaceae* was determined by counting CFUs on each plate and determined in duplicate and presented as CFU/mL BALF.

5.18. Identification of M. haemolytica in BALF

M. haemolytica-LPS lgG levels in BALF were measured according to manufacturer's instructions (BIO/K-139, Bio-X Diagnostics, Rochefort, Belgium). Negative and positive controls were provided by the same kit. The presence of *M. haemolytica*-LPS lgG was detected at 450 nm using a microplate reader (Bio-Rad Laboratories) and showed as the fold of the positive control.

DNA was extracted from BALF using PureLink Genomic DNA Mini Kit (Invitrogen) following the manufacturer's instructions. Real-time PCR methods for the detection of species-specific genes for *M. haemolytica* were performed using the primers and probes of BactoReal Kit (DVEB02911, Ingenetix GmbH, Vienna, Austria). BactoReal Kit detects the 16S rDNA gene of *M. haemolytica*. A probe-specific amplification-curve at 530 nm (FAM channel) indicates the amplification of *M. haemolytica* specific DNA.

Assay mix was prepared in a 20 μL volume that contained 10 μL of DNA Reaction Mix, 3 μL PCR grade water, 5 μL extracted DNA from samples, 1 μL primer, and 1 μL probe. Negative and positive controls were replaced by PCR grade water and positive *M. haemolytica*-DNA in the same kit, respectively. Real-time PCR was conducted on a Real-Time PCR Detection System (Bio-Rad Laboratories).

5.19. Histopathological lung scores

The right cranial lung lobe of calves (10 calves/treatment) was collected after slaughter at week 27. The collected lung lobe was immersed in 10% formalin for at least 24 h, after which it was embedded in paraffin. After paraffin embedding, 5 μm sections were cut and stained with HE according to standard methods. Four indications of lung lesions were examined by a treatment-blind observer, including 1) collapsed alveoli or thickened alveolar septa, 2) hyperplasia of bronchus or bronchioles, 3) infiltration of inflammatory cells, and 4) diapedesis of erythrocytes. Each section was classified according to a 4-point scale for lung lesions from a healthy lung (score 0) to severe lesions (score 3). Score 0 for no indication, score 1 for one indication, score 2 for two indications, and score 3 for three to four indications. Ten lung sections per calf were scored and scores were expressed as a mean value.

5.20. ELISA measurement

Levels of IL-8 (Mabtech, Nacka Strand, Sweden), IL-6 (Invitrogen), IL-1β (Invitrogen) or TNF-α (R&D Systems, Minneapolis, MN) in the supernatants of PBECs or in BALF and blood of calves were determined using ELISA kits according to manufacturer's instructions. IL-8 (R&D Systems) and IL-6 (BioLegend, San Diego, CA) release in the supernatants of A549 and 16HBE cells after different treatments were also measured by ELISA. The absorbance was measured at 450 nm using a microplate reader (Bio-Rad Laboratories).

5.21. Statistical analysis

Data from *in vitro* experiments were first checked for normality by using the Shapiro-Wilk normality test. After that, the parametric one-way ANOVA or two-way ANOVA with Tukey's *post hoc* test was performed for the analyses of *in vitro* parameters using GraphPad Prism 7.0 (GraphPad Software Inc., San Diego, CA). Results were considered statistically significant when $P < 0.05$ and considered a trend when $P < 0.10$.

Experimental results *in vivo* are expressed as non-transformed means ± SEM and analyzed for treatment and/or time effects with SAS 9.4 (SAS Institute Inc., Cary, NC), using the MIXED procedure unless otherwise indicated, including time as a repeated statement with calf as unit. For each parameter, the covariance structure was selected based on the lowest AIC and BIC. All analyses included a random effect of pen. For blood leukocyte concentration, the concentration at arrival (before application of the treatments) was included as a co-variable in the model. Studentized residuals of each model were checked visually on the homogeneity of variance and data were transformed if required to obtain homogeneity of variance. To evaluate differences between treatments, the contrast statement was used, and treatment differences were assessed per time-point separately. Clinical scores were assessed for treatment and time effects using the GLIMMIX procedure with a multinomial distribution including a random pen effect and potential differences between the treatments were evaluated using the contrast statement per timepoint. Pearson's correlations were applied for the relations within the inflammatory cytokines, *Pasteurellaceae* CFUs, and/or *M. haemolytica*-LPS lgG levels in BALF. The Chi-square test was performed for the positivity of *M. haemolytica* in calves. Differences were considered significant when $P < 0.05$ and considered a trend when $P < 0.10$.

Data availability

The data that support the findings of this study are available from the corresponding author upon reasonable request. Some data may not be made available because of privacy or ethical restrictions.

Credit author statement

Yang Cai: Conceptualization, Formal analysis, Investigation, Methodology, Visualization, Writing- original draft preparation. **Jos P.M. van Putten**: Methodology, Resources, Writing- Review & Editing. **Myrthe S. Gilbert**: Formal analysis, Investigation, Project administration, Writing- Review & Editing. **Walter J.J. Gerrits**: Conceptualization, Supervision, Funding acquisition, Writing- review & editing. **Gert Folkerts**: Conceptualization, Supervision, Funding acquisition, Writing-review & editing. **Saskia Braber**: Conceptualization, Methodology, Project administration, Supervision, Writing- review & editing.

Declaration of competing interest

The authors declare that they have no known competing financial interests or personal relationships that could have appeared to influence the work reported in this paper.

Appendix A. Supplementary data

Supplementary data to this article can be found online at https://doi.org/10.1016/j.biomaterials.2022.121461.

References

[1] S.J. Siegel, J.N. Weiser, Mechanisms of bacterial colonization of the respiratory tract, Annu. Rev. Microbiol. 69 (2015) 425–444.

[2] J.L. Caswell, Failure of respiratory defenses in the pathogenesis of bacterial pneumonia of cattle, Vet. Pathol. 51 (2) (2014) 393–409.

[3] R.A. Bem, J.B. Domachowske, H.F. Rosenberg, Animal models of human respiratory syncytial virus disease, Am. J. Physiol. Lung Cell Mol. Physiol. 301 (2) (2011) L148–L156.

[4] L. Van Driessche, B.R. Valgaeren, L. Gille, F. Boyen, R. Ducatelle, F. Haesebrouck, P. Deprez, B. Pardon, A deep nasopharyngeal swab versus nonendoscopic bronchoalveolar lavage for isolation of bacterial pathogens from preweaned calves with respiratory disease, J. Vet. Intern. Med. 31 (3) (2017) 946–953.

[5] M.M. Biesheuvel, G. van Schaik, N.M. Meertens, N.H. Peperkamp, E. van Engelen, E. van Garderen, Emergence of fatal Mannheimia haemolytica infections in cattle in The Netherlands, Vet. J. 268 (2021) 105576.

[6] K. Singh, J.W. Ritchey, A.W. Confer, Mannheimia haemolytica: bacterial-host interactions in bovine pneumonia, Vet. Pathol. 48 (2) (2011) 338–348.

[7] S. Ganesan, A.T. Comstock, U.S. Sajjan, Barrier function of airway tract epithelium, Tissue Barriers 1 (4) (2013), e24997.

[8] Y. Cai, S. Varasteh, J.P.M. van Putten, G. Folkerts, S. Braber, Mannheimia haemolytica and lipopolysaccharide induce airway epithelial inflammatory responses in an extensively developed ex vivo calf model, Sci. Rep. 10 (1) (2020) 13042.

[9] L.P. Datta, S. Manchineella, T. Govindaraju, Biomolecules-derived biomaterials, Biomaterials 230 (2020) 119633.

[10] Y. Cai, J. Folkerts, G. Folkerts, M. Maurer, S. Braber, Microbiota-dependent and -independent effects of dietary fibre on human health, Br. J. Pharmacol. 177 (6) (2020) 1363–1381.

[11] M. Asadpoor, C. Peeters, P.A.J. Henricks, S. Varasteh, R.J. Pieters, G. Folkerts, S. Braber, Anti-pathogenic functions of non-digestible oligosaccharides in vitro, Nutrients 12 (6) (2020) 1789.

[12] S. Arslanoglu, G.E. Moro, G. Boehm, Early supplementation of prebiotic oligosaccharides protects formula-fed infants against infections during the first 6 months of life, J. Nutr. 137 (11) (2007) 2420–2424.

[13] S. Arslanoglu, G.E. Moro, J. Schmitt, L. Tandoi, S. Rizzardi, G. Boehm, Early dietary intervention with a mixture of prebiotic oligosaccharides reduces the incidence of allergic manifestations and infections during the first two years of life, J. Nutr. 138 (6) (2008) 1091–1095.

[14] K.F. Budden, S.L. Gellatly, D.L. Wood, M.A. Cooper, M. Morrison, P. Hugenholtz, P. M. Hansbro, Emerging pathogenic links between microbiota and the gut-lung axis, Nat. Rev. Microbiol. 15 (1) (2017) 55–63.

[15] M. Asadpoor, S. Varasteh, R. Pieters, G. Folkerts, S. Braber, Differential Effects of Oligosaccharides on the Effectiveness of Ampicillin against Escherichia coli in Vitro, PharmaNutrition, 2021, p. 100264.

[16] M.J. Logtenberg, K.M.H. Donners, J.C.M. Vink, S.S. van Leeuwen, P. de Waard, P. de Vos, H.A. Schols, Touching the high complexity of prebiotic vivinal galacto-oligosaccharides using porous graphitic carbon ultra-high-performance liquid chromatography coupled to mass spectrometry, J. Agric. Food Chem. 68 (29) (2020) 7800–7808.

[17] P. Akbari, J. Fink-Gremmels, R. Willems, E. Difilippo, H.A. Schols, M.H. C. Schoterman, J. Garssen, S. Braber, Characterizing microbiota-independent effects of oligosaccharides on intestinal epithelial cells: insight into the role of structure and size : structure-activity relationships of non-digestible oligosaccharides, Eur. J. Nutr. 56 (5) (2017) 1919–1930.

[18] S.S. van Leeuwen, B.J.H. Kuipers, L. Dijkhuizen, J.P. Kamerling, Comparative structural characterization of 7 commercial galacto-oligosaccharide (GOS) products, Carbohydr. Res. 425 (2016) 48–58.

[19] S. Andrés-Lasheras, R. Zaheer, C. Klima, H. Sanderson, R. Ortega Polo, M.R. M. Milani, G. Vertenten, T.A. McAllister, Serotyping and antimicrobial resistance of Mannheimia haemolytica strains from European cattle with bovine respiratory disease, Res. Vet. Sci. 124 (2019) 10–12.

[20] Y. Gao, J. Wang, M. Chai, X. Li, Y. Deng, Q. Jin, J. Ji, Size and charge adaptive clustered nanoparticles targeting the biofilm microenvironment for chronic lung infection management, ACS Nano 14 (5) (2020) 5686–5699.

[21] E.S. Daniel Cozens, Miquel Lauder, Geraldine Taylor, Catherine C. Berry, Robert L. Davies, Pathogenic mannheimia haemolytica invades differentiated bovine airway epithelial cells, Infect. Immun. 87 (6) (2019), e00078-19.

[22] A.W. Confer, S. Ayalew, Mannheimia haemolytica in bovine respiratory disease: immunogens, potential immunogens, and vaccines, Anim. Health Res. Rev. 19 (2) (2018) 79–99.

[23] P. Ukkonen, K. Varis, M. Jernfors, E. Herva, J. Jokinen, E. Ruokokoski, D. Zopf, T. Kilpi, Treatment of acute otitis media with an antiadhesive oligosaccharide: a randomised, double-blind, placebo-controlled trial, Lancet 356 (9239) (2000) 1398–1402.

[24] D. Zopf, S. Roth, Oligosaccharide anti-infective agents, Lancet 347 (9007) (1996) 1017–1021.

[25] K.M. Craft, S.D. Townsend, Mother knows best: deciphering the antibacterial properties of human milk oligosaccharides, Acc. Chem. Res. 52 (3) (2019) 760–768.

[26] S.A. Chambers, R.E. Moore, K.M. Craft, H.C. Thomas, R. Das, S.D. Manning, S. G. Codreanu, S.D. Sherrod, D.M. Aronoff, J.A. McLean, J.A. Gaddy, S.D. Townsend, A solution to antifolate resistance in group B Streptococcus: untargeted metabolomics identifies human milk oligosaccharide-induced perturbations that result in potentiation of trimethoprim, mBio 11 (2) (2020), e00076-20.

[27] K.M. Craft, J.A. Gaddy, S.D. Townsend, Human milk oligosaccharides (HMOs) sensitize group B Streptococcus to clindamycin, erythromycin, gentamicin, and minocycline on a strain specific basis, ACS Chem. Biol. 13 (8) (2018) 2020–2026.

[28] A.B. Vishu Kumar, M.C. Varadaraj, L.R. Gowda, R.N. Tharanathan, Characterization of chito-oligosaccharides prepared by chitosanolysis with the aid of papain and Pronase, and their bactericidal action against Bacillus cereus and Escherichia coli, Biochem. J. 391 (Pt 2) (2005) 167–175.

[29] B.-K. Choi, K.-Y. Kim, Y.-J. Yoo, S.-J. Oh, J.-H. Choi, C.-Y. Kim, In vitro antimicrobial activity of a chitooligosaccharide mixture against Actinobacillus actinomycetemcomitans and Streptococcus mutans, Int. J. Antimicrob. Agents 18 (6) (2001) 553–557.

[30] M. Zeineldin, J. Lowe, B. Aldridge, Contribution of the mucosal microbiota to bovine respiratory health, Trends Microbiol. 27 (9) (2019) 753–770.

[31] D. Hagenfeld, T. Schulz, P. Ehling, T. Budde, U. Schumacher, P. Prehm, Depolarization of the membrane potential by hyaluronan, J. Cell. Biochem. 111 (4) (2010) 858–864.

[32] K. Shoaf, G.L. Mulvey, G.D. Armstrong, R.W. Hutkins, Prebiotic galactooligosaccharides reduce adherence of enteropathogenic Escherichia coli to tissue culture cells, Infect. Immun. 74 (12) (2006) 6920–6928.

[33] M. Quintero, M. Maldonado, M. Perez-Munoz, R. Jimenez, T. Fangman, J. Rupnow, A. Wittke, M. Russell, R. Hutkins, Adherence inhibition of Cronobacter sakazakii to intestinal epithelial cells by prebiotic oligosaccharides, Curr. Microbiol. 62 (5) (2011) 1448–1454.

[34] H.R. Sinclair, J. de Slegte, G.R. Gibson, R.A. Rastall, Galactooligosaccharides (GOS) inhibit Vibrio cholerae toxin binding to its GM1 receptor, J. Agric. Food Chem. 57 (8) (2009) 3113–3119.

[35] A. Sundarakrishnan, Y. Chen, L.D. Black, B.B. Aldridge, D.L. Kaplan, Engineered cell and tissue models of pulmonary fibrosis, Adv. Drug Deliv. Rev. 129 (2018) 78–94.

[36] R.G. Crystal, S.H. Randell, J.F. Engelhardt, J. Voynow, M.E. Sunday, Airway epithelial cells: current concepts and challenges, Proc. Am. Thorac. Soc. 5 (7) (2008) 772–777.

[37] P. Baral, S. Batra, R.L. Zemans, G.P. Downey, S. Jeyaseelan, Divergent functions of toll-like receptors during bacterial lung infections, Am. J. Resp. Crit. Care 190 (7) (2014) 722–732.

[38] Y. He, S. Liu, D.E. Kling, S. Leone, N.T. Lawlor, Y. Huang, S.B. Feinberg, D.R. Hill, D.S. Newburg, The human milk oligosaccharide 2'-fucosyllactose modulates CD14 expression in human enterocytes, thereby attenuating LPS-induced inflammation, Gut 65 (1) (2016) 33–46.

[39] S. Lehmann, J. Hiller, J. van Bergenhenegouwen, L.M. Knippels, J. Garssen, C. Traidl-Hoffmann, In vitro evidence for immune-modulatory properties of non-digestible oligosaccharides: direct effect on human monocyte derived dendritic cells, PLoS One 10 (7) (2015), e0132304.

[40] C.P. Sodhi, P. Wipf, Y. Yamaguchi, W.B. Fulton, M. Kovler, D.F. Nino, Q. Zhou, E. Banfield, A.D. Werts, M.R. Ladd, R.H. Buck, K.C. Goehring, T. Prindle Jr., S. Wang, H. Jia, P. Lu, D.J. Hackam, The human milk Oligosaccharides 2'-fucosyllactose and 6'-sialyllactose protect against the development of necrotizing enterocolitis by inhibiting toll-like receptor 4 signaling, Pediatr. Res. 89 (1) (2021) 91–101.

[41] Y. Cai, M.S. Gilbert, W.J.J. Gerrits, G. Folkerts, S. Braber, Galacto-oligosaccharides alleviate lung inflammation by inhibiting NLRP3 inflammasome activation in vivo and in vitro, J. Adv. Res. (2021), https://doi.org/10.1016/j.jare.2021.10.013.

[42] H. Janbazacyabar, J. van Bergenhenegouwen, K.A.T. Verheijden, T. Leusink-Muis, A. van Helvoort, J. Garssen, G. Folkerts, S. Braber, Non-digestible oligosaccharides partially prevent the development of LPS-induced lung emphysema in mice, PharmaNutrition 10 (2019) 100163.

[43] K.A. Verheijden, L.E. Willemsen, S. Braber, T. Leusink-Muis, P.V. Jeurink, J. Garssen, A.D. Kraneveld, G. Folkerts, The development of allergic inflammation in a murine house dust mite asthma model is suppressed by synbiotic mixtures of non-digestible oligosaccharides and Bifidobacterium breve M-16V, Eur. J. Nutr. 55 (3) (2016) 1141–1151.

[44] Y. Cai, M.S. Gilbert, W.J.J. Gerrits, G. Folkerts, S. Braber, Anti-inflammatory properties of fructo-oligosaccharides in a calf lung infection model and in mannheimia haemolytica-infected airway epithelial cells, Nutrients 13 (10) (2021), 3514.

[45] J.K. Pringle, L. Viel, P.E. Shewen, R.A. Willoughby, S.W. Martin, V.E. Valli, Bronchoalveolar lavage of cranial and caudal lung regions in selected normal calves: cellular, microbiological, immunoglobulin, serological and histological variables, Can. J. Vet. Res. 52 (2) (1988) 239–248.

[46] J.W. Allen, L. Viel, K.G. Bateman, S. Rosendal, P.E. Shewen, Cytological findings in bronchoalveolar lavage fluid from feedlot calves: associations with pulmonary microbial flora, Can. J. Vet. Res. 56 (2) (1992) 122–126.

[47] K. Ley, H.M. Hoffman, P. Kubes, M.A. Cassatella, A. Zychlinsky, C.C. Hedrick, S. D. Catz, Neutrophils: new insights and open questions, Sci. Immunol. 3 (30) (2018), eaat4579.

[48] C. Johansson, F.C.M. Kirsebom, Neutrophils in respiratory viral infections, Mucosal Immunol. 14 (4) (2021) 815–827.

[49] A. Craig, J. Mai, S. Cai, S. Jeyaseelan, Neutrophil recruitment to the lungs during bacterial pneumonia, Infect. Immun. 77 (2) (2009) 568–575.

[50] J.A. Whitsett, T. Alenghat, Respiratory epithelial cells orchestrate pulmonary innate immunity, Nat. Immunol. 16 (1) (2015) 27–35.

[51] U.S. FDA, Agency response letter GRAS notice GRN No. 236 [Galacto-oligosaccharides]. https://www.cfsanappsexternal.fda.gov/scripts/fdcc/index.cfm?set=GRASNotices&id=236, 2008. (Accessed 22 December 2021).

[52] U.S. FDA, Agency response letter GRAS notice GRN No. 620 [Galacto-oligosaccharides]. https://www.cfsanappsexternal.fda.gov/scripts/fdcc/index.cfm?set=GRASNotices&id=620, 2016. (Accessed 22 December 2021).

[53] P.R.C. NHC, National standard for use of food nutrition additives – GB14880-2012. https://www.cfsa.net.cn/Article/News.aspx?id=A05251ADFFF78E8C788FCC470652A4A9396920DB25238BD4D1A05A3F273DFE089D087A1FBEA144BA, 2012. (Accessed 22 December 2021).

[54] N.F. EFSA Panel on Nutrition, F. Allergens, D. Turck, T. Bohn, J. Castenmiller, S. De Henauw, K.I. Hirsch-Ernst, A. Maciuk, I. Mangelsdorf, H.J. McArdle, A. Naska, Safety of the extension of use of galacto-oligosaccharides as a Novel food pursuant to Regulation (EU) 2015/2283, EFSA J. 19 (10) (2021), e06844.

[55] T. Kobayashi, N. Yasutake, K. Uchida, W. Ohyama, K. Kaneko, M. Onoue, Safety of a novel galacto-oligosaccharide: genotoxicity and repeated oral dose studies, Hum. Exp. Toxicol. 28 (10) (2009) 619–630.

[56] S.E. Ladirat, H.A. Schols, A. Nauta, M.H.C. Schoterman, F.H.J. Schuren, H. Gruppen, In vitro fermentation of galacto-oligosaccharides and its specific size-fractions using non-treated and amoxicillin-treated human inoculum, Bioact. Carbohydr. Diet. Fibre 3 (2) (2014) 59–70.

[57] K. van Leenen, L. Van Driessche, L. De Cremer, C. Masmeijer, F. Boyen, P. Deprez, B. Pardon, Comparison of bronchoalveolar lavage fluid bacteriology and cytology in calves classified based on combined clinical scoring and lung ultrasonography, Prev. Vet. Med. 176 (2020) 104901.

[58] S. Amat, T.W. Alexander, D.B. Holman, T. Schwinghamer, E. Timsit, Intranasal bacterial therapeutics reduce colonization by the respiratory pathogen mannheimia haemolytica in dairy calves, mSystems 5 (2) (2020), e00629-19.

[59] J. Baruch, N. Cernicchiaro, C.A. Cull, K.F. Lechtenberg, J.S. Nickell, D.G. Renter, Performance of multiple diagnostic methods in assessing the progression of bovine respiratory disease in calves challenged with infectious bovine rhinotracheitis virus and Mannheimia haemolytica1, J. Anim. Sci. 97 (6) (2019) 2357–2367.

[60] S.M. McGuirk, S.F. Peek, Timely diagnosis of dairy calf respiratory disease using a standardized scoring system, Anim. Health Res. Rev. 15 (2) (2014) 145–147.

[61] G. Caldow, Bronchoalveolar lavage in the investigation of bovine respiratory disease, In Pract. 23 (1) (2001) 41–43.

[62] S. Eid, S. Marouf, H.Y. Hefny, N.M. Al-Atfeehy, Pasteurellaceae members with similar morphological patterns associated with respiratory manifestations in ducks, Vet. World 12 (12) (2019) 2061–2069.